IMPARTING ELECTRICAL CONDUCTIVITY INTO ASPHALT COMPOSITE USING GRAPHITE

A Thesis

by

AISHWARYA BARANIKUMAR

Submitted to the Office of Graduate Studies of
Texas A&M University
in partial fulfillment of the requirements for the degree of

MASTER OF SCIENCE

Chair of Committee,	Philip Park
Committee Members,	Nasir Gharaibeh
	Mohammad Naraghi
Head of Department,	John Niedzwecki

August 2013

Major Subject: Civil Engineering

ABSTRACT

Electrically conductive asphalt composites have immense potential for various multifunctional applications such as self-healing, self-sensing, snow and ice removal, and energy harvesting, and controlling asphalt conductivity is the first step to enable such applications. Previous investigators have used conductive fibers as major conductive additive for asphalt composites, and the sudden transition from the insulated phase to the conductive phase, known as the percolation threshold, is commonly observed. Since the percolation threshold hinders precise control of asphalt conductivity, it is imperative to mitigate the sudden transition in the electrical resistivity curve to enable practical applications of asphalt composites. Some recent publications showed the potential of graphite in mitigating the sudden transition. The study presented herein investigates possibility of precisely controlling the electrical conductivity of asphalt concrete only by adding filler size graphite powder. Nine different types of graphite having different particle shapes and sizes are selected to investigate their effect on conductivity control. The volume resistivity of the asphalt mastic specimens containing various concentrations of graphite is evaluated. In addition, scanning electron microscope analysis is conducted for the graphite particles to provide physical explanation for their different effects on imparting conductivity. The results show that the electrical resistivity of asphalt mastic is significantly varied with the types of graphite. The mastics containing natural flake graphite show gradual decrease in volume resistivity as the graphite content increases, and sufficiently low resistivity can be

obtained in the specimens with natural flake graphite. On the other hand, amorphous graphite is not efficient in reducing volume resistivity. Graphite with high surface area presents difficulty in mixing. In the next stage of research, two best performing graphite out of the nine different types are selected to be added to asphalt concrete, and the effect of aggregates on electrical resistivity is examined. It is found that flake graphite 516 provides good electrical conductivity along with improved mechanical performance of asphalt concrete. Thus the study provides fundamental information on the selection of graphite type and amount to achieve proper electrical conductivity required for multifunctional applications.

DEDICATION

To My Father, G. Baranikumar,

to My Mother, B. Malini,

to My Sister, B. Rupanjali

for their kind support, love and patience.

ACKNOWLEDGEMENTS

I take this opportunity to sincerely thank my academic advisor, Dr. Philip Park for his guidance, moral support, and kind co-operation throughout my Master's Program. His encouragement and belief in my abilities to work motivated me to successfully complete my research tasks. I truly believe that Dr. Park's suggestions and work ethic has transformed me into a more professional researcher and further extended my desire to achieve high standards in work quality.

I would like to express my thanks to my committee members, Dr. Nasir Gharaibeh and Dr. Mohammad Naraghi for their time, valuable suggestions and most of all their cooperation in helping me finish my work in a swift manner. It was my pleasure to have them on my committee.

I wish to whole heartedly thank my beloved friend Narain Hariharan for his help and support throughout my stay at Texas A&M University.

A special thanks to my team members, Abdul Kabbara and Xijun Shi, without whom I would not have been able to complete my laboratory experiments.

I want to extend my gratitude to the Southwest Region University Transportation Center (SWUTC) for their financial support and trust in my research. Thanks to the Asbury Carbons Inc. and Knife River for providing their materials, graphite and aggregates respectively for use in this research.

Texas A&M University has provided me with excellent facilities and an opportunity to interact and learn from distinguished professors and eminent scholars. I

am fortunate and blessed to pursue my Master's degree at this prestigious academic institution. I thank all the teaching staff at Texas A&M University for their unwavering dedication in pursuit of transferring their knowledge and transforming me and my fellow Aggies to shine in our respective professional careers.

I am extremely thankful to all my friends at the Materials and Pavements division in Texas A&M for their friendship and continued encouragement. Special thanks to Lorena and Fan Yin for guiding me with laboratory tasks and helping me with technical issues pertaining especially to asphalt concrete mix designs.

Finally, love and regards to my family for their encouragement, patience and care.

TABLE OF CONTENTS

Page

LIST OF FIGURES

Page

LIST OF TABLES

Page

1. INTRODUCTION

Asphalt concrete is a composite material that is extensively used in the construction of highways, airport runways, and parking lots. Riding comfort, durability, and water resistance are some of the driving mechanical characteristics making it the most preferred choice in the pavement industry.

Multifunctional materials have the simultaneous ability to exhibit non-structural functions apart from their regular structural functions (Gibson 2010). Structural materials can be designed multifunctional by integrating electrical, magnetic, optical, and possibly other functionalities that exhibits advantages beyond the sum of the individual capabilities. Materials of this kind have tremendous potential to be utilized as smart materials impacting future structural performance by improving efficiency and safety. Electrical conductivity is one of the popular non-structural properties in construction materials, and Figure 1 shows the concept of multifunctional construction materials utilizing electrical conductivity.

Asphalt concrete has possibilities of being used as a multifunctional material by controlling its electrical conductivity. Asphalt concrete, by nature, is a non-conductive composite material, but its conductivity can be improved by using conductive additives.

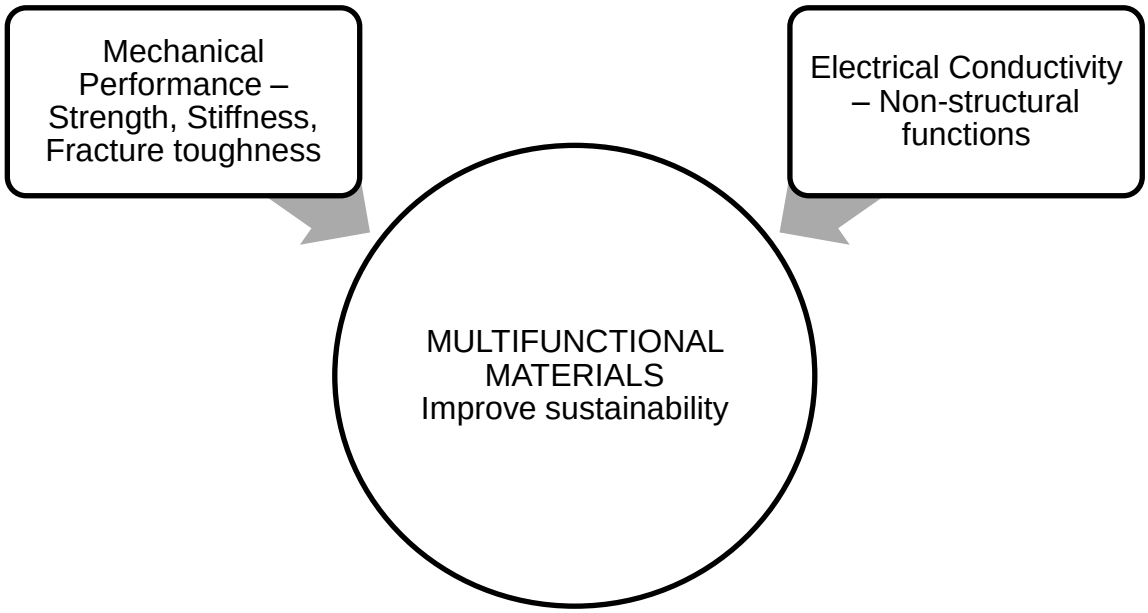

Figure 1. Multifunctional materials with mechanical and electrical functions

1.1 Background

The concept of electrically conductive asphalt concrete was initiated by Minsk in 1968, and this topic has gained immense interest in the last decade resulting in increased number of publications. These efforts have largely been motivated by the potential benefits of utilizing electrical properties of asphalt composites. For instance, the electrical heating applications of conductive pavements have been studied to remove snow and ice (Xiangyang et al. 2010). Electric heating of conductive asphalt pavements is also expected to promote self-healing by reducing the rest period. In addition, piezo-resistivity of conductive asphalt, which refers to change in electrical resistivity with applied mechanical pressure, can be used for self-sensing of strain (Liu and Wu 2009).

Self-sensing of damage for evaluating pavement distress is possible if the relationship between the electrical property and internal damage is provided. Moreover, fiber type conductive additives can improve the durability of asphalt concrete, thereby increasing the service life of the pavement systems and making them sustainable (Park 2012).

The possible non-structural applications of electrically conductive asphalt concrete and the associated benefits are presented in Figure 2.

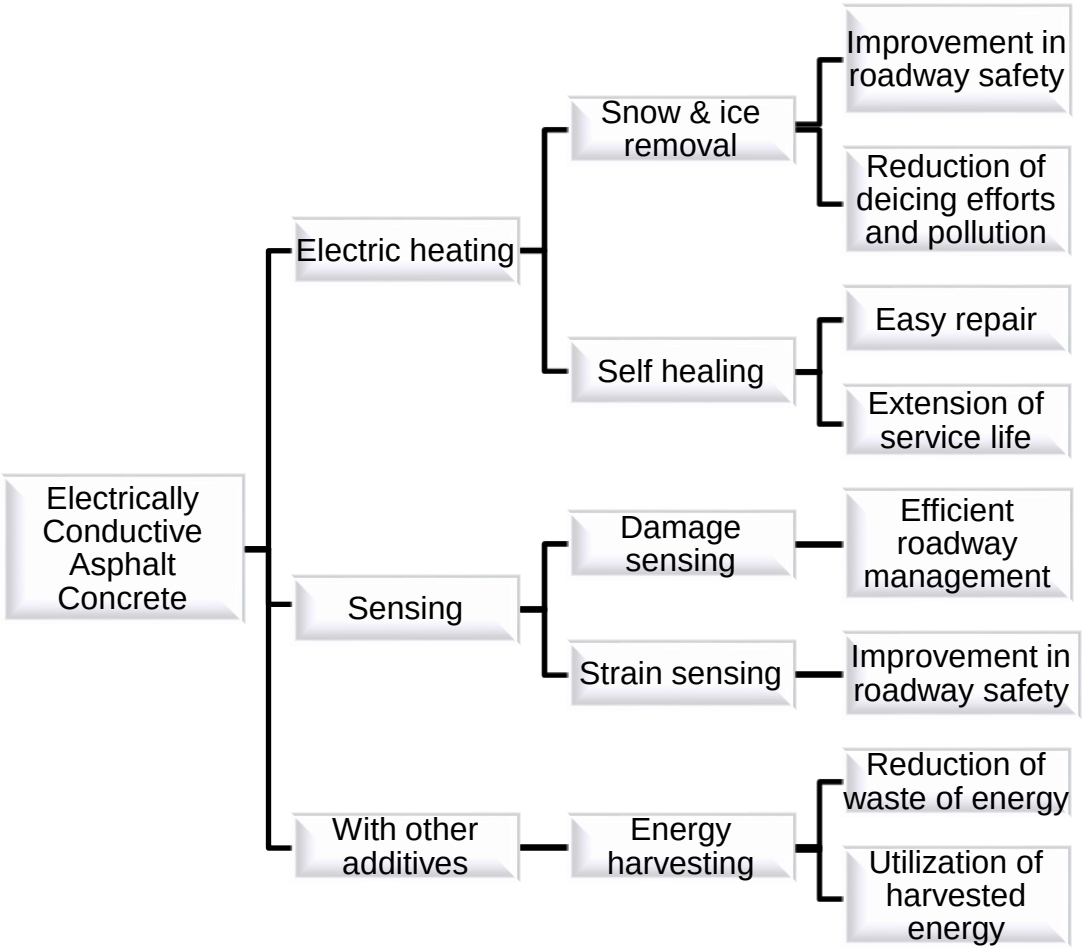

Figure 2. Possible benefits of electrically conductive asphalt concrete

1.2 Problem Statement

In order to utilize the full spectrum of applications of electrically conductive asphalt composites discussed in the previous section, a precise control of the volume resistivity of the composites is needed.

Previous investigators have tried to make asphalt concrete electrical conductive by adding different conductive fillers and fibers such as micro-steel fibers (Huang et al. 2006 and Serin et al. 2012), carbon fibers (Wu et al. 2005), steel wool (Garcia et al. 2009), carbon black (Wu et al. 2005), and graphite powder (Wu et al. 2005; Garcia et al. 2009). Most of the previous investigators selected the fiber type additives as their primary conductive additives rather than powder types because relatively smaller amount of fibers are needed to improve conductivity than graphite or carbon black (Huang et al. 2006). However, the following shortcomings were observed in using conductive fibers:

- Percolation threshold is a sudden transition from the insulated to the conductive phase, and was a common observation in asphalt composites containing conductive fibers (Wu et al. 2005 and Garcia et. al 2009). The sudden resistivity drop inhibits precise control of conductivity, and limits the potential applications of conductive pavements. Therefore, gradual resistance change with increase of conductive additive is favorable as illustrated in Figure 3.
- Due to the physical dimensions of fibers, mixing the fibers with asphalt concrete proved to be a challenge. Controlling the dispersion of fibers and ensuring

uniform dispersion throughout the mix was difficult (Huang et. al 2009). This may lead to inhomogeneous resistivity within the specimens.

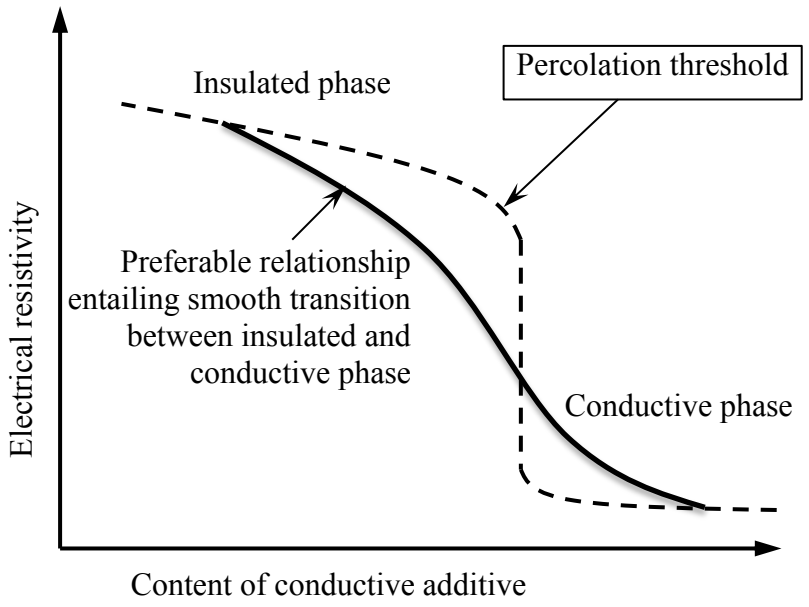

Figure 3. Electrical resistivity transition curve

Graphite is one of the powder type conductive additives used as supplementary material by some investigators (Huang et al. 2006; Garcia et al. 2009; Liu and Wu 2011b). While the above mentioned difficulties are prevalent with fiber type conductive additives, the use of graphite powder ensures relatively easy mixing and uniform dispersion. More importantly, the percolation threshold might be mitigated when using graphite powder even though large quantities than the conductive fibers are needed to reduce the electrical resistivity (Huang et al. 2009 and Mo et al. 2005). On the other hand, the efficiency of graphite in imparting conductivity is not consistent in the previous publications due to the use of different types of graphite by different

researchers. None of the researchers till date have studied the effect of different graphite types on imparting the electrical conductivity. This motivated the present study to experiment with variety of graphite types and identifying the best graphite that improves conductivity with a smooth resistivity transition.

1.3 Research Objectives

The goal of the study is to investigate the effect of graphite types on imparting electrical conductivity in asphalt composites. The following objectives will be achieved through the course of this research:

1. To study electrical conductivity of asphalt mastic (asphalt binder + fillers including graphite) using nine different types of graphite.
2. Reason out the difference in results through comparison with SEM images of the graphite.
3. To control electrical conductivity of asphalt concrete (asphalt mastic + aggregate) with the most efficient graphite types selected from the asphalt mastic tests.

1.4 Thesis Outline

The thesis is divided into six sections. Each section has been briefly described below:

Section 1 introduces the topic of research and provides background information on electrically conductive asphalt composites. The problem statement is defined and the research objectives are outlined.

Section 2 presents a comprehensive literature review in this field along with the objectives and results obtained by various researchers. This section also provides information on multifunctional materials and discusses in depth the applications of conductive asphalt concrete.

Section 3 characterizes the different types of graphite used for the research with their properties and scanning electron microscope (SEM) images. The SEM images are used to provide physical explanation to their effect in conductivity results.

Section 4 describes the experimental procedures and electrical conductivity results of asphalt mastic specimens containing different types and concentrations of graphite. The relationships between the conductivity and contents of various graphite types are obtained to sort out the most efficient graphite type.

Section 5 outlines the electrical conductivity of asphalt concrete fabricated with the two most efficient graphite types. The effect of these conductive fillers on mixing and compaction, percent air-voids, indirect tensile strength are also discussed in this chapter.

Section 6 presents the conclusion of the research along with recommendations for future work.

2. LITERATURE REVIEW

A review of literatures pertinent to imparting and controlling conductivity in asphalt concrete and the various possible applications of multifunctional materials are summarized in the this section.

2.1 Approaches to Impart Conductivity into Asphalt Concrete

The interest in imparting electrical properties into asphalt concrete dates back to 1970s. Minsk (1971) first patented "Electrically conductive asphaltic concrete" using graphite as a conductive medium for the purpose of melting snow and ice on roadway surfaces. Stratfull (1974) and Fromm (1976) used coke-breeze from steel industry to produce conductive hot-mix asphalt (HMA) for cathodic protection of steel rebars in concrete bridges. Zaleski et al. (1998) patented a pavement system containing electrically conductive layer for de-icing purpose. They utilized graphite and coke as conductive additives. Parallel to asphalt concrete, extensive study on electrically conductive Portland cement concrete have been published. Barnard (1965) patented electrically conductive (cementitious) concrete, and since then, various efforts were reported on the widened applications of conductive concrete (Chung 2003).

Findings from numerous research studies in the past have shown that electrical conductivity of asphalt concrete can be improved with the addition of conductive fillers and/or fibers. Wu et al. (2003) proved that the inclusion of graphite beyond a critical content decreases the resistivity of asphalt-based composites. In this paper, the authors focused mainly on the self-sensing ability of conductive asphalt. In 2005, electrical

conductivity of asphalt concrete with other additives such as carbon black (CB), graphite (G) and carbon fibers (CF) were investigated by Wu et al. (2005). It was found that pure carbon fiber modified asphalt concrete showed the best performance in conductivity followed by graphite and carbon black as illustrated in Figure 4. In the figure, the content of conductive additive is presented as volume percentage of the binder phase of the mixture. The electrical resistivity was found to decline rapidly when specific amounts of conductive additives were added, which is called percolation threshold. Previous investigators (Wu et al. 2005; Huang et al. 2006) explained that a three-dimensional conductive network is established at percolation threshold, and hence improvement in conductivity is not significant after this point. Wu et al. (2005) thus concluded that the desired electrical resistivity can be obtained by keeping the content of conductive additives slightly above the optimum (percolation) level, but making sure that it should not go beyond to minimize the influence on mechanical properties of asphalt concrete.

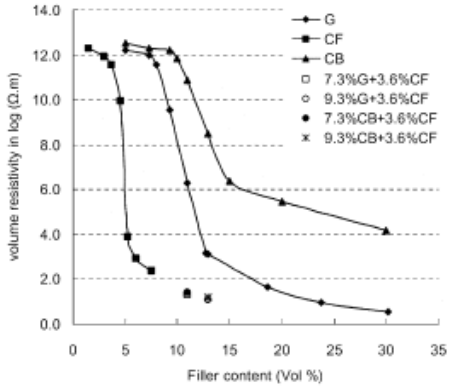

Figure 4. Effect of type of conductive additives on the resistivity of asphalt concrete (Wu et al. 2005)

Similar studies were carried out by a research team at University of Tennessee. Huang et al. (2006) investigated the different options for producing electrically conductive asphalt. Micro-scale steel fibers (8 μm in diameter and 6 mm in length), aluminum chips (passing 0.10 mm sieve), and graphite (passing 0.075 mm sieve) were examined for their ability in imparting conductivity. It was observed that the aluminum chips are not effective in increasing electrical conductivity of the mixture in spite of being an excellent conductive material. The reason was that aluminum gets easily oxidized in air forming aluminum oxide, which has low conductivity. While aluminum is not the right choice for practical purpose, the mixtures with micro-scale steel fibers and graphite exhibited good electrical conductivity. Resistivity in order of $10^3\Omega$.m was reached with the addition of 0.33% steel fibers by volume of asphalt binder. Approximately 2.3% graphite by volume of asphalt binder was needed to obtain the similar resistivity level. Variation in electrical conductivity during fatigue evolution was also studied through indirect tensile test (IDT) and beam fatigue tests.

Huang et al. (2009) extended their investigation to the mechanical performance of conductive asphalt composites. Dynamic Shear Rheometer (DSR) test were conducted to study the effect of conductive additives, i.e., micro-scale steel fibers, carbon fibers and graphite; on the viscoelastic properties of asphalt mastic (mixture of asphalt binder and conductive additives). The results show that with increase in the content of the conductive additives, the complex shear modulus, G^*, increased. This implies that the conductive additives can stiffen asphalt binder. High contents of graphite were required to achieve sufficiently low resistivity, and hence the stiffness of the mastic was

improved to a great extent. The mechanical performances of conductive HMA mixtures were investigated through IDT and dynamic modulus tests. Though graphite reduces the IDT strength of the mixtures, it improves the dynamic modulus. On the other hand, the fracture energy of the mixtures with carbon or steel fibers was slightly improved due to the reinforcing effect of the fibers. Figure 5 depicts the IDT strength and dynamic modulus of asphalt concrete containing various additives.

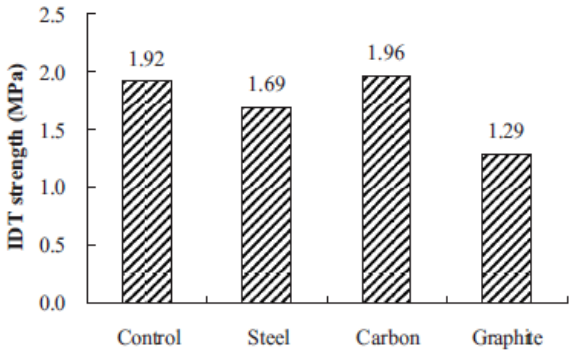

(a) IDT strength for various additives

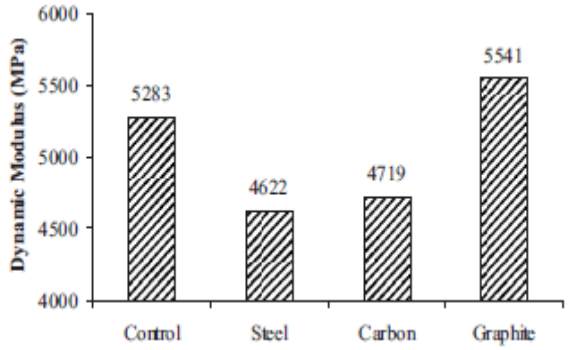

(b) Dynamic Modulus at 10 Hz

Figure 5. Mechanical performance of HMA mixture with conductive additives (Huang et al. 2009)

A comprehensive study was conducted by Garcia et al. (2009). The effect of fiber content, sand–bitumen ratio and the combination of fillers and fibers (graphite and steel wool) on the resistivity of asphalt mortar were examined. The authors divided the changes in the resistivity with volume percentages of conductive additive into four different phases: the insulated phase, transition phase, conductive phase, and excess of fibers phase. The insulated phase is where the fibers are not connected with one another and the resistivity is approximately equal to that of plain asphalt concrete. The transition phase is where the percolation path of fibers forms and the resistivity drops rapidly leading to the next phase called the conduction phase. Beyond the conductive phase, named as the excess of fibers phase, the reduction in length of conductive paths is not significant any more, and electrical resistivity of the composite decreases slightly with increase in fiber content. In addition, it becomes difficult to mix when clusters of fibers start forming with large proportions of fibers. Figure 6 depicts this theory in a schematic fashion.

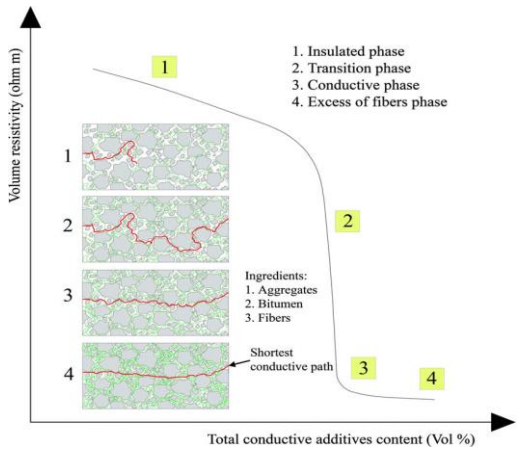

Figure 6. Schematic representation of volume resistivity versus fiber content (Garcia et al. 2009)

According to Garcia et al. (2009), the resistivity of the composite material varied not only with the content of conductive additives, but also with sand-bitumen ratio. It was observed that there exists an optimum conductive particles-bitumen ratio for each sand-bitumen ratio where the resistivity of the mixture reached a minimum. By reducing the sand-bitumen ratio below the optimum content, the resistivity was found to increase exponentially, making the material non-conductive. Interestingly, the resistivity increases even for a higher sand-bitumen ratio than the optimum level. Figure 7 shows the optimum sand-bitumen ratios for different amount of conductive additives. It should be noted that graphite significantly reduces the optimum sand-bitumen ratio when it is combined with steel wool.

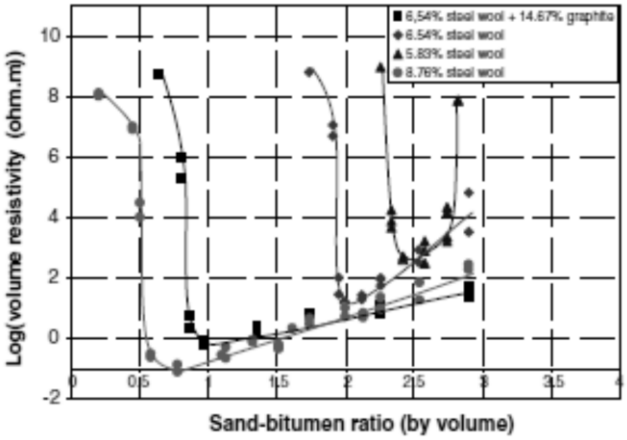

Figure 7. Variation in electrical resistivity with sand-bitumen ratio (Garcia et al. 2009)

In addition, Liu et al. (2008) and Liu and Wu (2009) investigated the piezoresistivity of conductive asphalt concrete. Piezoresistivity is an electrical property

that the electrical resistivity of a material changes due to applied stress or strain. It reflects the microstructural change in the material on application of load. This phenomenon was observed in conductive asphalt, and it implies that conductive asphalt has a possibility of being utilized as a self-sensing material. Such a smart material can sense its own damage or strain and monitor its structural health condition. A constant compressive stress of 0.7 MPa was applied to the specimens, and changes in resistance along with the compressive strain were noted. The relationship between electrical property and mechanical condition broadens the possible multifunctional application of conductive asphalt.

The mechanical characteristics of conductive asphalt concrete using graphite and carbon fiber were investigated by Wu et al. in 2010. They studied the indirect tensile strength, indirect tensile resilient modulus, and indirect tensile fatigue life of conductive asphalt concrete. The results indicated that conductive asphalt concrete has higher tensile strength than regular asphalt concrete in dry condition, but has lower wet tensile strength and tensile strength ratio (TSR). This means the conductive asphalt concrete has relatively lower resistance to water, but fortunately the ratio is higher than the minimum required value. The indirect tensile resilient modulus increases with the addition of conductive components. The effect of carbon fibers on indirect resilient modulus is more prominent than that of graphite. The results of the indirect tensile fatigue test show that the fatigue life of conductive asphalt concrete at higher stress levels is greatly enhanced when it is compared to regular asphalt concrete. Figure 8 summarizes the findings of Wu et al. (2010)

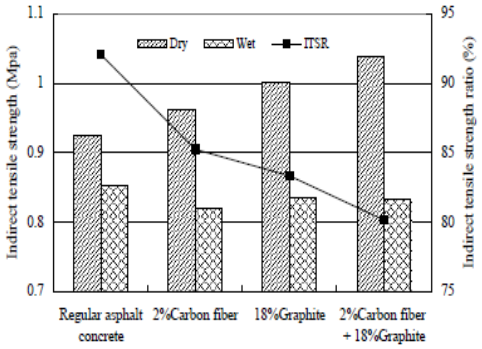

(a) Indirect tensile strength results for regular and conductive asphalt

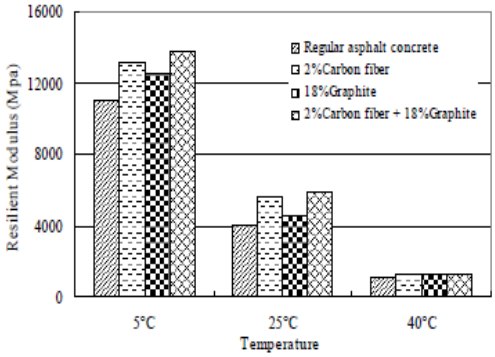

(b) Indirect tensile resilient modulus results at different temperatures

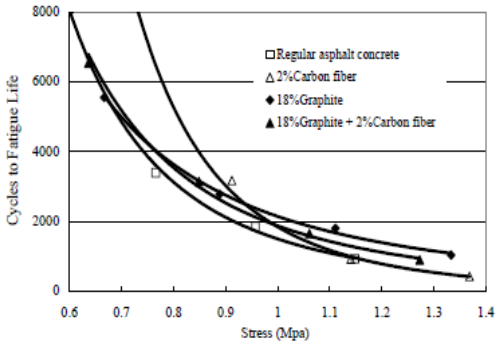

(c) Indirect tensile fatigue life graph for regular and conductive asphalt composites

Figure 8. Mechanical test results of conductive asphalt concrete (Wu et al. 2010)

Similar study on the IDT strength of porous asphalt concrete with steel fibers was conducted by Liu et al. (2010b). It was observed that the IDT strength of the mixture increases with the increase of steel fibers until a certain content. Beyond that, more addition of fibers reduces the thickness of mastic film around the aggregates leading to poor adhesion. This reduces the IDT strength of porous asphalt concrete. Figure 9 shows the results of IDT test on conductive porous asphalt concrete.

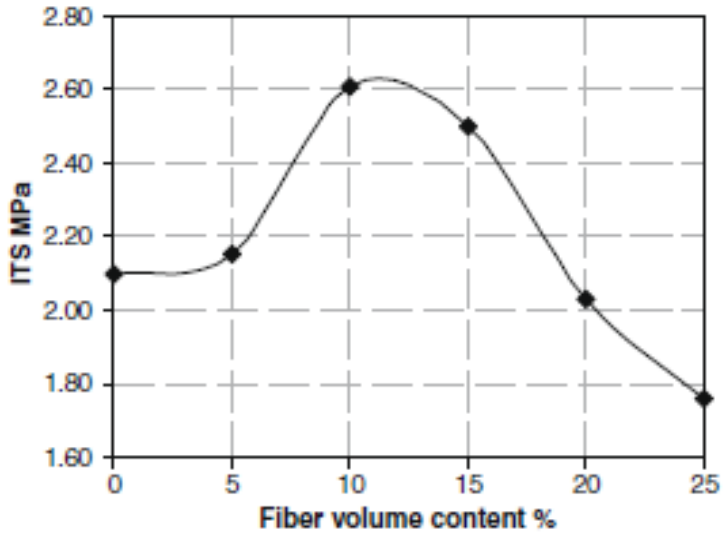

Figure 9. The indirect tensile strength on conductive porous asphalt concrete (Liu et al. 2010b)

Liu and Wu (2011a) investigated the variation of Marshall Stability, resilient modulus, and dynamic stability of graphite and carbon fiber modified asphalt concrete. According to Liu and Wu (2011a), the addition of graphite did not considerably enhance the mechanical strength of asphalt concrete.

They concluded that graphite can be good conductive filler, but its lubricating property caused by weak bond between plain hexagonal crystal structures of graphite might impair the mechanical properties of asphalt concrete.

Park (2012) studied the effect of graphite powders on imparting electrical conductivity in asphalt mastic and showed that the electrical resistivity significantly varied with the type (shape and size) of graphite.

Clearly, as reviewed above, electrically conductive asphalt concrete has become popular during last ten years.

Table 1 summarizes the previous research on conductive asphalt. As compared in the Table 1, the amount of conductive additives required for specific resistivity varies significantly with the investigators. For example, volume percentage of graphite at 10^3 Ω.cm ranges from 11% to 30%. Therefore, the causes of this variability and the factors affecting conductivity of asphalt mixtures should be clarified for precise conductivity control.

Table 1. Summary of research on conductive asphalt composites

Authors	Conductive Fillers Used	Percentage of additives to attain resistivity of 10^3 Ω.cm (% vol. by binder)	Purpose
Minsk (1968)	Graphite (G)	G- 17% and 21%	Snow and ice removal
Stratfull (1974)	Coke-breeze	---	Cathodic protection of steel rebars in concrete bridges
Fromm (1976)	Coke-breeze	---	Cathodic protection of concrete bridge decks
Zaleski et al. (1998)	Graphite and coke	---	De-icing purpose
Wu et al. (2003)	Graphite	G- 26%	Self-sensing applications
Wu et al. (2005)	Carbon black (CB), graphite, carbon fibers (CF)	CB- 13%, CF- 6% or G-30%	Imparting conductivity CF>G>CB
Huang et al. (2006)	Micro-scale steel fibers (SF), aluminum chips and graphite	SF -0.75% or G-11%	Study conductivity, IDT and beam fatigue test
Huang et al. (2009)	Micro-scale steel fiber, carbon fiber and graphite	SF- 0.99%, CF- 5% or G-18%	IDT strength, IDT fracture energy, Dynamic modulus, Flow number, APA rut depth
Garcia et al. (2009)	Graphite and steel wool (SW)	SW- 6% or G- beyond 30%	Sand-bitumen ratio, effect of fiber content
Liu and Wu (2009)	Graphite and carbon fiber	G-12%	Piezo-resistivity
Wu et al. (2010)	Graphite and carbon fiber	G-22% or CF- beyond 8%	IDT, indirect tensile fatigue life
Liu and Wu (2011a)	Graphite and carbon fiber	G-15%	Marshall stability, resilient modulus and dynamic stability
Park (2012)	Graphite	G -21%	Electrical conductivity of different types of graphite

2.2 Multifunctional Applications of Conductive Asphalt Concrete

Multifunctional materials are considered to be smart and innovative materials due to their widespread technological impact and ability to respond to external stimuli in an environment friendly manner. The technology necessary to build the next-generation devices like autonomous robots, smart homes, intelligent sensors, structural health monitoring, and smart transportation system is expected to be centered on multifunctional materials.

The concept of developing multifunctional materials stems from the need to accomplish multiple applications and performances in a single system. The sought-after characteristics of these materials include energy efficient non-structural functions, such as self-sensing, self-healing, and electromagnetic properties, in addition to traditional structural functions, such as stiffness and strength. Hence, the research and development involved in multifunctional materials faces a great technological challenge with limitless applications. Interdisciplinary investigations have been carried out for the molecular structure and non-structural properties of various materials to explore multifunctional possibilities and to extend their use across different disciplines.

Some of the potential multifunctional applications of conductive asphalt concrete include electrical heating, sensing, and energy harvesting. These features are discussed below for a more thorough understanding of the benefits.

Electric Heating

Snow and ice removal

One of the major issues in the society was to improve the transportation safety under freezing and/or snowy weather. Removing snow and ice, especially on highway and bridge surfaces is a crucial step to enhance transportation safety. Materials such as salt or sand can be used to remove ice from pavement (Blackburn 2004). Salt is most popular deicing agent since it is inexpensive and efficient. However, ice will not be melted by salt or similar deicing agents at extremely cold temperature. Furthermore, deicing chemicals have obvious negative impacts including the concrete corrosion and environmental pollution, and these problems are paid much attention by International Energy Agency (IEA) and World Health Organization (WHO) (Lofgren 2001; Sanzo and Hecnar 2006). Snow and ice on the conductive asphalt pavement can be removed by electric heating, which is a process of converting electric energy to heat (Chen et al. 2012). This process ensures reliable deicing and reduced pollution.

Self-healing

Asphalt concrete is a self-healing material (Little and Bhasin 2007). Once the load causing microcracks is removed, the molecules on either side of each crack starts diffusing to the other end, and the microcracks are healed with time. The time required for this healing process is called rest period. The challenge arises when the traffic flow is too heavy to allow sufficient rest period for self-healing. One of the solutions is to increase the temperature of asphalt concrete because the healing can be accelerated with increase of temperature (Bonnaure et al. 1982; Daniel and Kim 2001). Liu et al. (2010a;

2010b; 2010c) and Garcia showed the possibility of promoting self-healing by induction electrical energy into conductive asphalt concrete. Garcia et al. (2011) and Liu et al. (2010a; 2010b; 2010c) suggested a non-contact electric heating technique using electromagnetic field. In this method, a coil is placed over the conductive asphalt specimen and a power supply is connected to the coil. As alternating current flows through the coil, the electromagnetic field is created which induces current (eddy current) in the conductive specimen below the coil. The induced current dissipates heat in the specimen by Joule effect. Figure 10 shows the test set-up of induction heating presented in Liu et al (2010b).

Figure 10. Test set-up for induction heating (Liu et al. 2010b)

Sensing

Strain and damage sensing

A self-sensing material can monitor its own strain and damage without an external sensor. Thus, compared to structural health monitoring system based on the attached sensor network (extrinsic), self-sensing structural materials are intrinsically

smart. The intrinsically smart structures have possible advantages than extrinsically smart structures due to their low cost, good durability, large sensing volume, and absence of mechanical property degradation due to the embedding of sensors (Chung and Wang 2003).

As was discussed earlier on description of percolation threshold theory, the contact resistance between the filler materials governs the resistivity of the asphalt or cementitious composites. Upon application of an external compressive load, the filler particles get closer resulting in decreased resistivity (Wen and Chung 2007). Such a change in resistivity with application of mechanical stresses is referred as piezoresistivity (Wu et al. 2006). This is the mechanism by which conductive asphalt pavements sense their own structural health.

Energy Harvesting

Research conducted by Mallick et al. (2008) and Lee and Correia (2010) has shown that energy on the surface of pavement can be harvested. Pyroelectricity, thermoelectricity, and piezoelectricity are possible electrical functions that can be utilized for the energy harvesting, and conductive asphalt concrete is expected to contribute to activate these probable functions.

3. SCANNING ELECTRON MICROSCOPE ANALYSIS

This section introduces physical properties of the various graphite powders used in the research. The properties including density, particle size, surface area, etc. are discussed below. These properties play a major role in deciding the mixing and compaction difficulties of conductive asphalt concrete. Scanning electron microscope images of the graphite are also presented to provide an explanation on the observed conductivity variation with the graphite types.

3.1 Types of Graphite

Nine different types of graphite were obtained from Asbury Carbons Inc. to study their effect on imparting conductivity into asphalt composites. While the ideal shape of graphite particle is hexagonal, the shape and size varies depending on the source and manufacturing process. The graphite types are classified as three flake types (F146, F516 and F3204), two amorphous types (505 and 508), one artificial type (A99), two types with ultra-high surface area (SA4827 and TC307), and carbon black (5303). The properties of these graphite types are presented in Table 2.

Table 2. Properties of graphite (Asbury Carbons Inc.)

Asbury ID	% Carbon	Typical Size (μm)	Density	Surface area (m^2/g)	Typical Resistivity (Ω·cm)	Price ($/lb)	Note
F146	96.86	20.22 (< 44)	True density = 2.32 (g/cc)	6.35	-	$1.27	Flake type
F3204	97.05	14.7 (< 44)	-	7.41	-	-	Flake type
F516	95.45	- (< 212)	-	-	-	-	Flake type
505	84.50	- (< 75)	-	-	-	-	Amorphous type
508	81.77	16.27 (< 44)	-	-	-	$0.64	Amorphous type
A99	99.68	22.82	True density = 2.22 (g/cc)	8.47	0.047	$1.01	Artificial type
SA4827	99.66	1.64	-	248.92	0.184	$4.47	Artificial type Ultra high surface area
TC307	99.92	2.59	True density = 2.16 (g/cc)	352	-	-	Artificial high surface area type
5303	99.90	0.03	True density = 1.8 (g/cc)	254	0.341	$7.87	Carbon black

* Abbreviations – F: flake, A: artificial, SA: surface area
* Density of Graphite = 2.267 (g/cc)
* Typical Resistivity (Asbury): Natural Flake: 0.036-0.088 (Ω·cm)

Particle size and shape can affect mixture properties in various ways. For instance, particle size of TC307 (352 m^2/g) is small resulting in very high surface area. This implies that TC307 will require more binder to coat its particles than other graphite. Therefore, the mixture with TC307 is expected to have poorer mechanical performance than the other mixtures when the same amount of binder is used.

3.2 Scanning Electron Microscope Analysis

SEM images of the graphite powders listed in Table 2 were taken to investigate the shape of the graphite particles. Figure 11a – 11i shows the SEM images of the nine graphite powders. In Figure 11, a magnification scale of 2000 was fixed for all images.

As shown in Figure 11a, 11f, and 11h, the flake graphite has thin plate shape particles which may allow super-conductivity of electrons through the surface of flat surface. The amorphous and artificial graphite types, on the other hand, have irregular shapes. Mixing of the high surface area graphite and carbon black were very difficult. Their particle sizes are very fine, and great content of binder may be required to coat its surface.

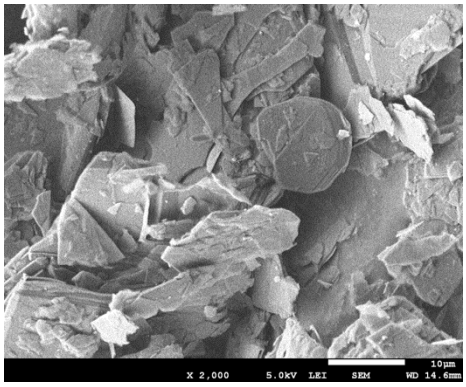

(a) Flake Graphite F146

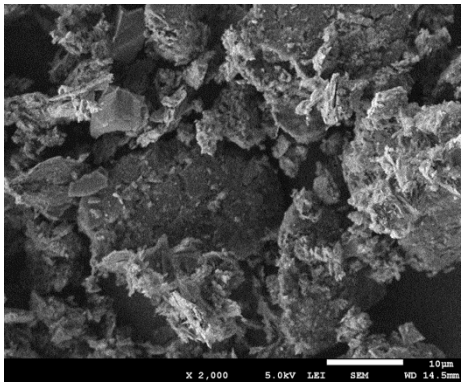

(b) Amorphous Graphite 505

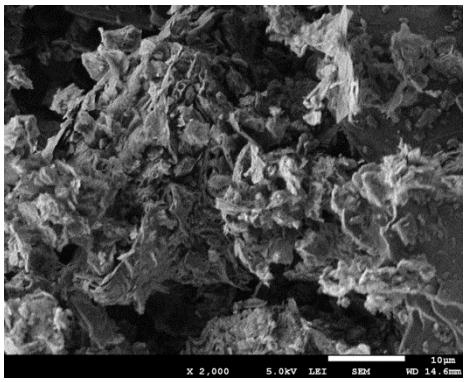

(c) Artificial Graphite A99

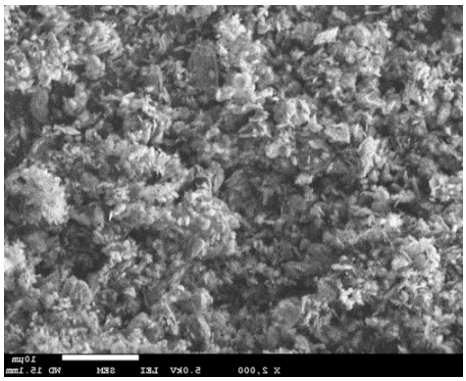

(d) Ultra-High Surface area Graphite SA4827

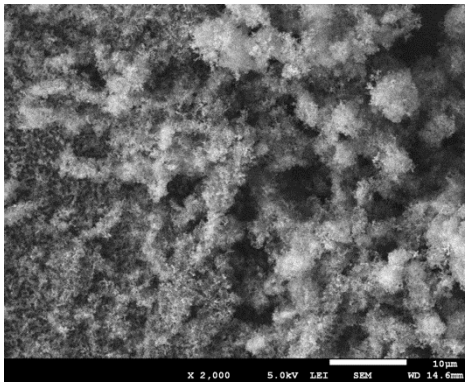

(e) Carbon Back 5303

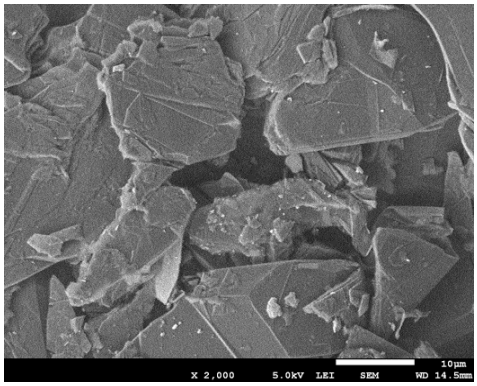

(f) Flake Graphite F516

Figure 11. SEM images of graphite powders

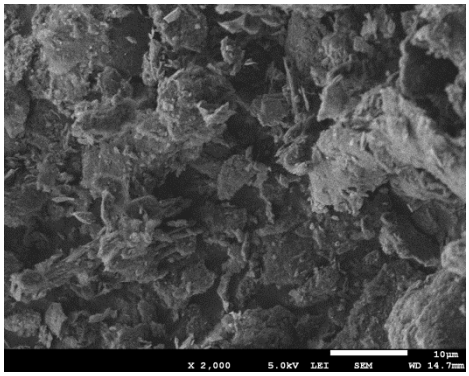

(g) Amorphous Graphite 508

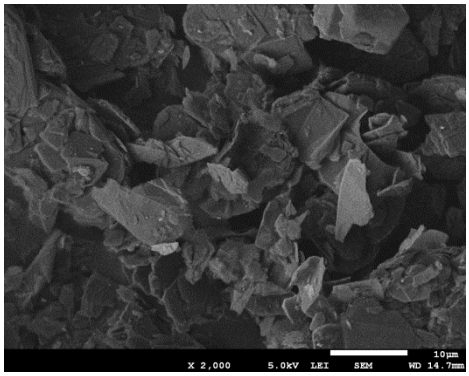

(h) Flake graphite 3204

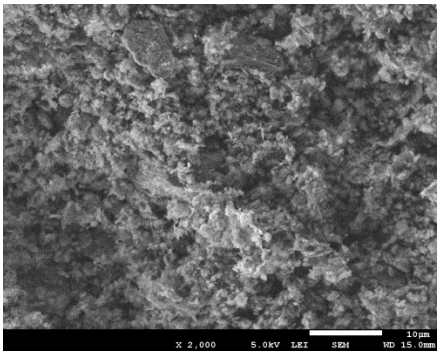

(i) High-Surface area Graphite TC307

Figure 11. SEM images of graphite powders (Continued)

4. ELECTRICAL CONDUCTIVITY OF ASPHALT MASTIC

4.1 Introduction

The literature review of this thesis has highlighted the possible applications of electrically conductive asphalt and some of those attempts by previous investigators. Steel wool, steel fibers, carbon fibers and some anonymous types of graphite have been used as the conductive additives to impart conductivity. The present study focuses solely on the effect of various types of graphite on imparting conductivity of asphalt composites.

Previous investigations using graphite have shown promising results for precise conductivity control – gradual drop in resistivity with increasing graphite contents. In this section, asphalt mastic test procedure, specimen preparation, and their test results are discussed. In addition, mixing difficulties observed in certain graphite types are explained.

4.2 Experimental Set-up

Asphalt mastic specimens were prepared using PG70-22 asphalt binder (ASTM 2007a) and various combinations of conductive and non-conductive fillers. The density of binder is 1.032 g/cm^3.

Asphalt mastics specimens are composed of 50% asphalt binder and 50% filler by weight of total mastic. This proportion was kept constant throughout the experiment. Type II Portland cement was used as the non-conductive traditional filler. Conductive fillers, graphite, replace part of cement filler in the mastic specimens ranged from 10%

to 50% by weight of the mastic. For example, when the graphite content is 20%, cement content is 30% to maintain the proportion of filler in the mastic.

The mastic specimens were prepared in thin film shape as shown in Figure 12a. Dry pine wood was used as a base for spreading asphalt mastic. The wooden base blocks were coated with heat resistant epoxy to prevent absorption of asphalt binder. The wood, binder, and filler were conditioned at 150 ºC for 2 hours in the oven before mixing. Once the materials were heated, the binder and filler (combination of cement and graphite with various proportions) were mixed manually by hand for 3-5 minutes to ensure uniform and complete dispersion of the filler in the mastic. The mastic was then spread on the epoxy-coated wooden blocks and conditioned again at 150 ºC for 1 hour. The average thickness of mastic was computed by reading the weight of the wooden block before and after spreading the mastic. Once the weight of mastic on the wooden block was found, it was divided by the density of mastic and the spread area to obtain its average thickness. The density of the mastic was estimated using the individual densities of the binder, cement, and graphite and their respective weight proportions in the mastic. For each type and content of graphite, three mastic specimens were prepared to improve reliability of the results.

The mastic specimens were conditioned at room temperature for 8 hours before testing. Copper tapes were installed at every 50 mm distance and used as electrodes (Figure 12a). Silver paste was painted between the mastic and copper tapes to ensure full contact between them. Two-point sensing method was used to measure impedance of the mastic specimens. The copper tapes at various locations on the specimen enabled to

select different combinations of electrodes, i.e., distance between electrodes can be 50 mm, 100 mm, or 200 mm, to observe the impedance change with distance.

Solartron 1260A and 1296 (Impedance/Gain Phase Analyzer, Figure 12b) were used to measure the resistance of the specimens. Solartron 1260A can measure resistance only up to 100 MΩ. Solartron 1296 was combined with 1260A to extend the measurable range up to 100 TΩ. Electrical impedances of the specimens were measured at 0.1V with AC frequency sweep ranged from 0.01 Hz to 1000 Hz. Once the resistances were obtained, the volume resistivity was calculated using the equation (1) below:

$$\rho = R\,\frac{A}{L} \tag{1}$$

where, ρ is the volume resistivity measured in Ω-cm; R is the resistance in Ω obtained from the experiment; A is the cross-sectional area of the mastic in cm^2; and L is the distance between the electrodes in cm. The electric field is assumed to be constant and end effect is assumed to be negligible.

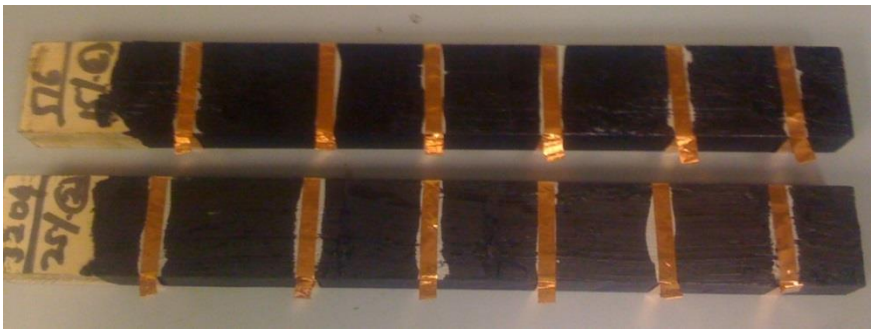

(a) Mastic specimens

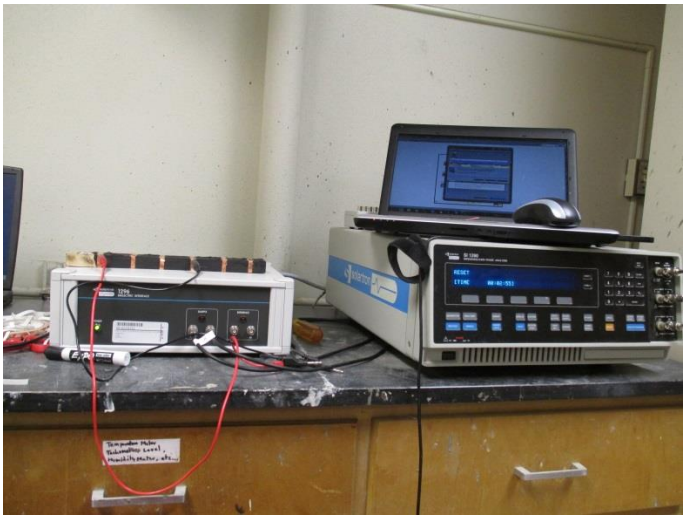

(b) Resistivity measurement set-up: Solartron 1296 & 1260A

Figure 12. Experimental set-up

4.3 Electrical Conductivity Results

Figure 13 shows an example of the frequency sweep data for the specimens with different concentrations of F146 graphite. It can be observed that the resistance gradually decreases with increasing contents of graphite. At 10% and 20% of F146 graphite, the mastics have low conductivity, and the resistance values are not steady with the frequency. In contrast, at 25% and higher content of F146 graphite, the asphalt mastics

show steady resistances, and show step-wise decrease in resistance with increase of graphite content.

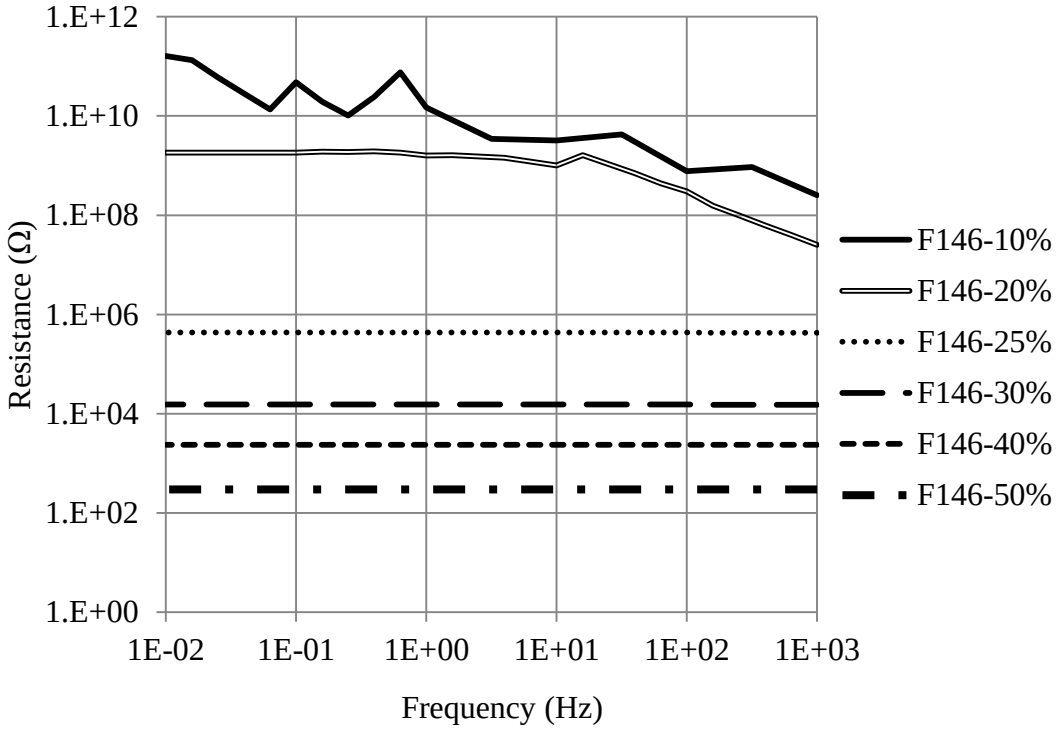

Figure 13. Variation in resistance over frequency sweep for F146

Figure 14 compares the resistances of mastics with six different graphite types at 40% content by weight over the frequency range. It is clear from the figure that the mastic resistance varies with the types of graphite. The specimens with F516 and F146 graphite display the lowest conductivity, whereas the mastics with 505 and 508 graphite still remain non-conductive at 40% content. These results can be compared with the particle shape of graphite observed from the SEM analysis. The thin plate shape of flake

type graphite particles is similar to the ideal crystal structure of graphite, and allows super-conductivity through the surface of the flat surface. On the other hand, the irregularity on the amorphous graphite particles seems to work as a barrier against the flow of electron, leading to poor conductivity. This graph demonstrates the importance of selecting the proper type of graphite for imparting conductivity.

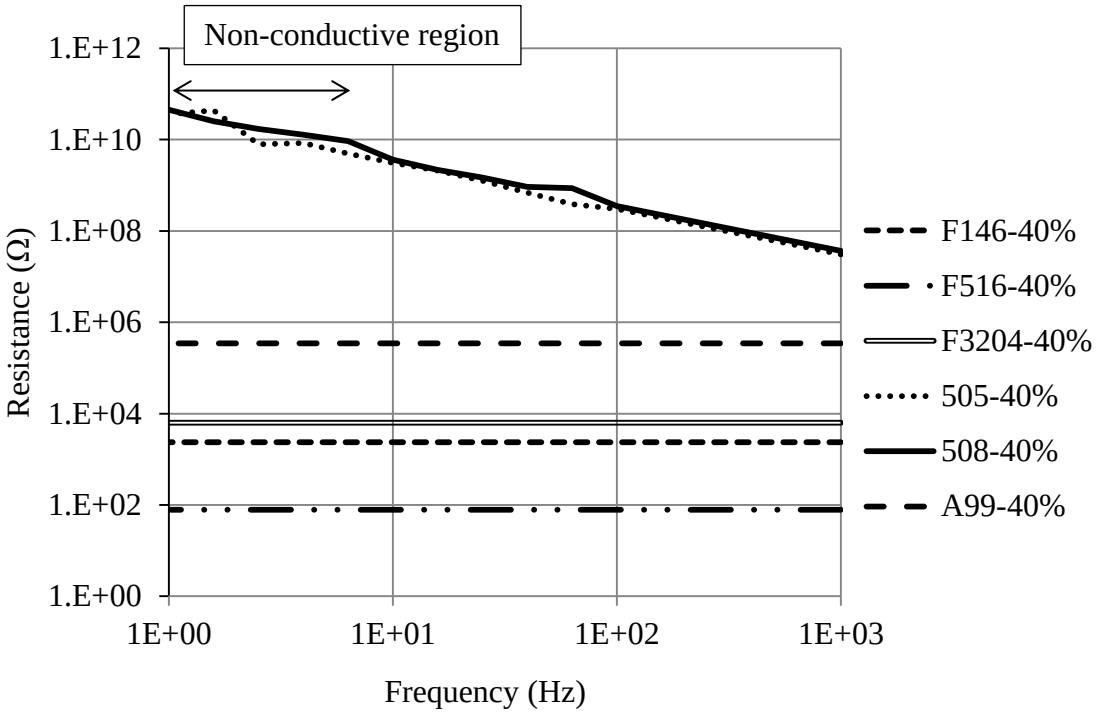

Figure 14. Variation in resistance over frequency sweep for different conductive fillers

Figure 15 compares the variation of conductivity with the content of two contrasting graphite types: flake type F146 and amorphous type 505 graphite.

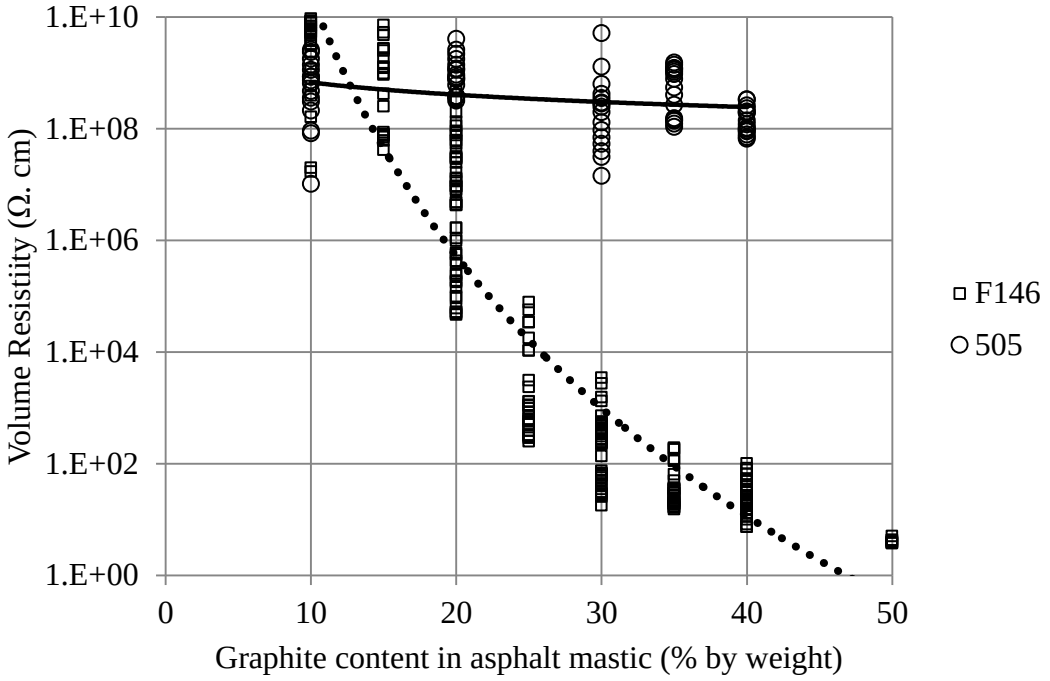

Figure 15. Comparison of volume resistivity of flake and amorphous graphite types

A gradual drop in the resistivity is observed with the increasing concentrations of F146 graphite fillers in the mastic. Since there is no sudden resistivity drop, it is difficult to specify percolation threshold which is common in the case of fiber-added asphalt mixtures. The electrical resistivity of each of the graphite is presented in Appendix A1. Approximately 24 readings were obtained for each mastic specimen.

The measured electrical resistivity of all cases is summarized in Figure 16. Each dot in the figure represents the average value of twenty-four volume resistivity readings. The first noticeable observation is the similar trend in resistivity of all the flake type graphite. As the contents of flake type graphite increase, the resistivity drops up to

sufficiently low with gradual manner. This shows the possibility of precise conductivity control with the flake type graphite.

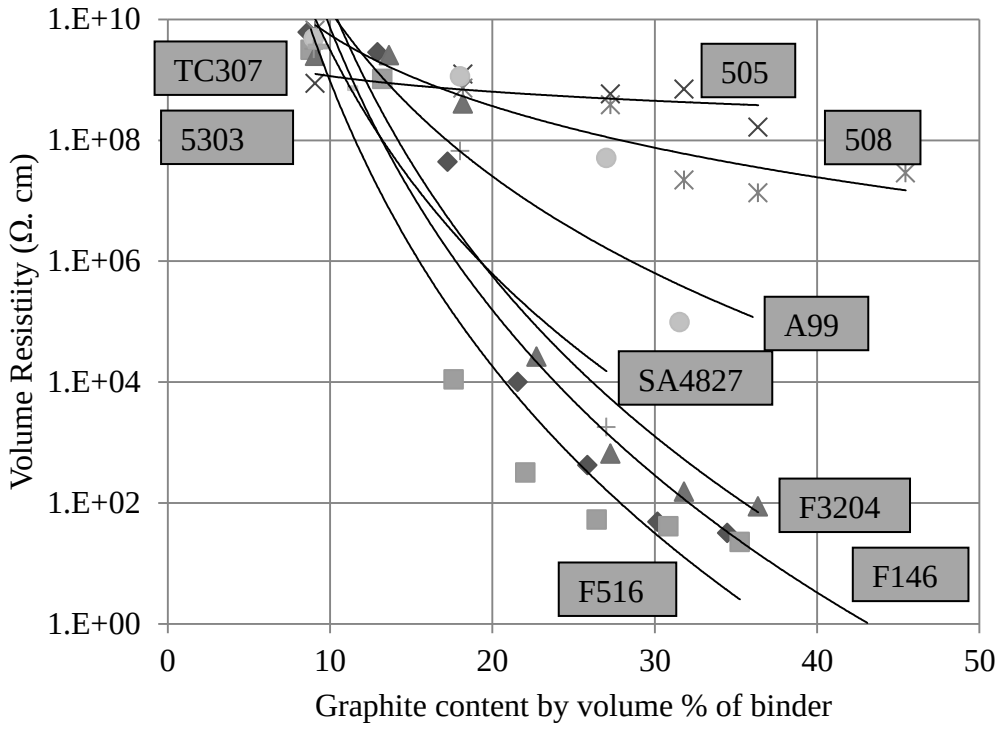

Figure 16. Comparison of volume resistivity of various graphite types

The Amorphous and Artificial type graphite are not good enough to improve conductivity, and the specimens have very low conductivity even at higher contents of those graphite.

4.4 Effects on Mixing

Mixing difficulty was observed with the high surface area graphite. Specimens with SA4827 graphite were prepared up to 30% graphite content because of the mixing

issue. TC307 and 5303 were even harder to mix, and specimens with only 10% content of graphite fillers were prepared. The mastic becomes thick and sticky beyond a certain concentration. This limits the use of this type of graphite and their effect on conductivity could not be studied further. The mastics containing flake type graphite, F146, F516, and F3204, became sticky as the concentration increases, but no significant difficulty in mixing was observed up to high concentration. The artificial type A99 produced a watery mix which was easier to spread on the woods than other graphite. In contrast, the amorphous type 505 and 508 were difficult to mix beyond graphite content of 30%.

5. ELECTRICAL CONDUCTIVITY OF ASPHALT CONCRETE

5.1 Introduction

Asphalt concrete is most common material used for pavement surfaces, airport runways, and bridge decks. Asphalt concrete is made up of asphalt binder, aggregate, and air void. Traditional asphalt concrete is a good insulator by nature with resistivity ranging from 10^9-10^{11} Ω.cm (Wu et al. 2003). As discussed in section 2, conductivity of asphalt concrete can be improved with conductive additives, and conductive asphalt concrete has various potential applications such as self-healing, de-icing, traffic monitoring and so on.

From the experiments with asphalt mastics containing various graphite, two best preforming graphite are selected to study their effect on asphalt concrete. This section presents the mix design, specimen preparation, test method, and test results on conductive asphalt concrete.

5.2 Experimental Set-up

Materials and Mix Design

Asphalt concrete specimens were prepared using PG70-22 asphalt binder (density 1.032 g/cc). The specimens were prepared in accordance with the Superpave mixture design method. The aggregate gradation used for the mixture is shown in Table 3. The optimum binder content was determined to be 5.3% by weight of total mixture by Superpave method (see Appendix A3). The aggregate included 35% crushed limestone (coarse aggregate), 60% river sand (fine aggregate) and 5% filler. The specific gravities

of coarse aggregate, fine aggregates, and filler are measured as 2.57 g/cc, 2.63 g/cc, and 3.15 g/cc, respectively. The proportion of coarse and fine aggregates was selected to satisfy D-6 mixture requirements specified in ASTM 2001. The sieve analysis results of fine and coarse aggregates are presented in Appendix A2.

Table 3. Aggregate gradation

Sieve size (mm)	19	12.5	9.5	4.75	2.36	1.18	0.6	0.3	0.15	0.075
% passing	100	99.9	95.3	68.1	50.8	35.3	21.0	11.5	7.2	6.1

The volumetric properties of the control mixture, i.e., the specimen without graphite, are listed in Table 4.

Table 4. Volumetric properties of the mixture

AC (%)	G_{mm} (g/cc)	G_{mb} (g/cc)	Air Voids (%)	VMA	VFA
5.3	2.427	2.328	4.0	16.5	75.2

This mixture design was kept constant for the specimens containing graphite too. While the content of graphite (conductive filler) varied, 5% of filler content in the mixture was kept constant by adjusting the amount of non-conductive cement filler.

Based on the mastic test results, F146 and F516 graphite were selected for the mixture. The contents of graphite were 20%, 25%, and 30% by weight of asphalt mastic, i.e., 2.1%, 2.6%, and 3.1% by weight of total mix, respectively.

Specimen Preparation

The specimen preparation and volumetric analysis were conducted in accordance with Superpave mixture design and ASTM standards.

The aggregates and fillers were heated at 150 ºC for at least 4 hours to eliminate moisture, and the binder was heated for 2 hours at the same mixing temperature prior to mixing. The fillers were mixed with aggregates first, and then the binder was added. A mechanical mixer was used to mix the materials until the aggregates and fillers were coated well with the binder. The mixture was then conditioned in the oven at the compaction temperature (135 ºC).

Superpave Gyratory compactor was employed to compact the specimens. Cylindrical specimens with 150 mm diameter and 95 mm height were compacted with gyration until the percent air void reach target value (4%). The compacted specimens are shown in Figure 17. For each test case, four cylindrical specimens were prepared: three for measuring indirect tensile strength and one for measuring the electrical conductivity. The specimen for electrical conductivity was drilled to make three core cutting samples out of it. This cutting will eliminate the error in conductivity measurement by removing the conductive mastic coated on the side of the specimens.

Figure 17.Compacted asphalt concrete specimens

Electrical Resistivity Measurement Set-up

Copper tapes were installed as electrodes at the top and bottom of the core-cut specimens. A highly conductive silver paste was painted between the specimen surface and copper tape to maintain the full contact between them. Solartron 1260A and 1296 (Impedance/Gain Phase Analyzer) were used to measure the resistance of the specimens. The resistance was then converted to volume resistivity corresponding to the dimensions of the specimen. The specimens and measurement set-up are shown in Figure 18.

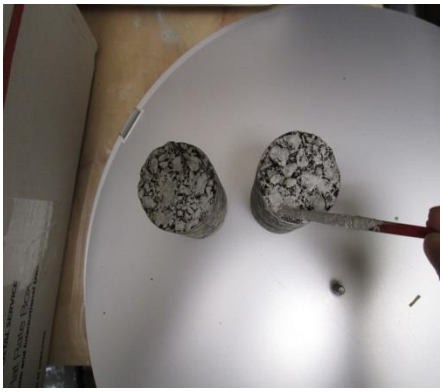

(a) Painting silver paste on top and bottom surfaces of specimens

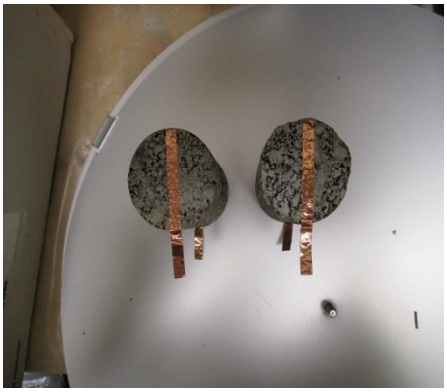

(b) Installing copper tapes as electrodes

(c) Electrical resistivity measurement devices: Solartron 1260A and 1296.

Figure 18. Asphalt concrete specimens and electrical resistance devices

Indirect Tensile Strength Test

The three compacted specimens were conditioned at room temperature (25 ºC) before testing. Instron 5583 was used for performing the indirect tensile strength test. During the IDT test, monotonic compressive load was applied on the specimen at a

constant displacement rate of 50.8 mm/min (2 in. /min) until fracture. The load and strain were recorded. The IDT strength was computed as follows:

$$S_T = \frac{2 \text{ x } P}{\pi \text{ x } t \text{ x } D} \quad (2)$$

where, S_T is the IDT strength in MPa, *P* is the maximum load in N, *t* is the specimen height immediately before test in mm, and *D* is the specimen diameter in mm. The test was performed in accordance with ASTM 2007c. The IDT test set-up and the fractured specimen are shown in Figure 19.

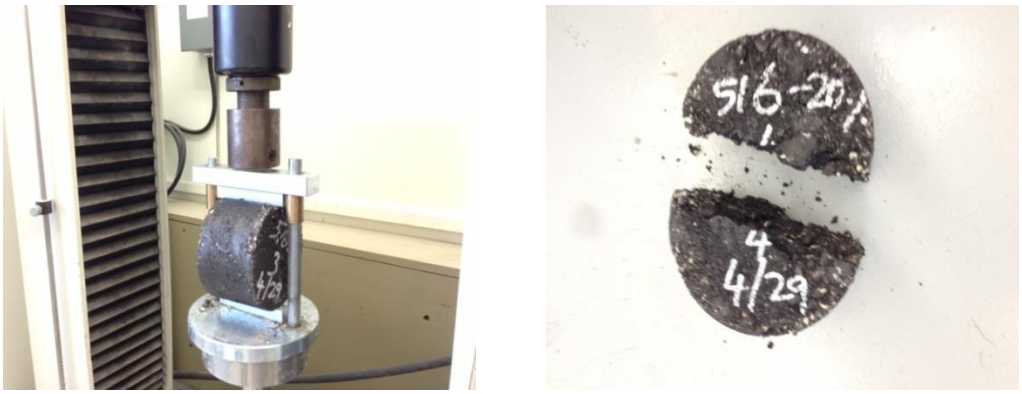

(a) IDT test (b) Specimen after IDT test

Figure 19. Indirect tensile strength experiment

5.3 Experimental Results

Volumetrics

Four specimens for each case were prepared, and their volumetric properties were evaluated. Table 5 provides the average values of these volumetric properties.

Table 5. Volumetric properties of all specimens

Specimens	AV	G_{sb}	G_{mm}	G_{mb}	VMA	VFA
Control Mix	4.09	2.642	2.428	2.329	16.52	75.27
146-20%	4.01	2.625	2.394	2.298	17.09	76.57
146-25%	4.14	2.621	2.411	2.311	16.50	74.92
146-30%	4.60	2.617	2.427	2.315	16.22	71.65
516-20%	4.38	2.624	2.389	2.285	17.55	75.01
516-25%	4.19	2.620	2.402	2.302	16.79	75.07
516-30%	4.10	2.615	2.386	2.288	17.14	76.09

It should be to be noted that most of the specimens have air-void (AV) in the range 4±0.5% (ASTM 2005). G_{sb} is the specific gravity of aggregates (coarse+ fine+ filler) in the mix. G_{sb} decreases with increase in contents of graphite because the density of graphite is smaller than that of cement. G_{mm} and G_{mb} are the theoretical and bulk specific gravity of the mixture, respectively, measured in accordance with ASTM 2003 and 2007b. The voids in mineral aggregate (VMA) and voids filled with asphalt (VFA) are calculated from the equations shown below:

$$\mathrm{VMA} = 100 - \frac{\mathrm{Gmb} \times \mathrm{Ps}}{\mathrm{Gsb}} \quad (3)$$

$$\mathrm{VFA} = 100 \times \frac{\mathrm{VMA} - \mathrm{AV}}{\mathrm{VMA}} \quad (4)$$

where, Ps is the percentage of aggregates in the total mixture, and AV is the percent air-voids.

Table 6 compares number of gyrations needed to obtain 4% target AV for the specimens with various graphite contents. The control mixture has 56 gyrations, and the number of gyrations increases with increase of graphite content. It seems that graphite absorbs more binder, and hence the mixture becomes dry and sticky. This shows that the mixtures with graphite require extra care in compaction.

F146 and F516 show similar trend in compaction effort. But the mixtures with F516 require less number of gyrations to achieve the target air-void than the mixtures with F146 when the same amount of graphite is added.

Table 6. Average number of gyrations for different mixes

Specimens	Number of Gyrations
Control Mix	56
146-20%	48
146-25%	110
146-30%	232
516-20%	77
516-25%	98
516-30%	127

Electrical Resistivity Test

Figure 20 shows the variation of volume resistivity of asphalt concrete specimens with conductive filler contents. Each dot in the figure refers to the average of three volume resistivity readings for each case. Volume resistivity of the control mixture (no graphite) is $5.3x10^{10}\Omega.cm$. The specimens with the two types of conductive graphite

(F146 and F516) show similar trend to the mastic test results – resistivity decreases with increase in graphite content. The volume resistivity's of asphalt concrete specimens are around 10 times higher than that of mastic specimens because of the additional non-conductive volume of aggregate. The detailed electrical resistivity results are presented in Appendix A4.

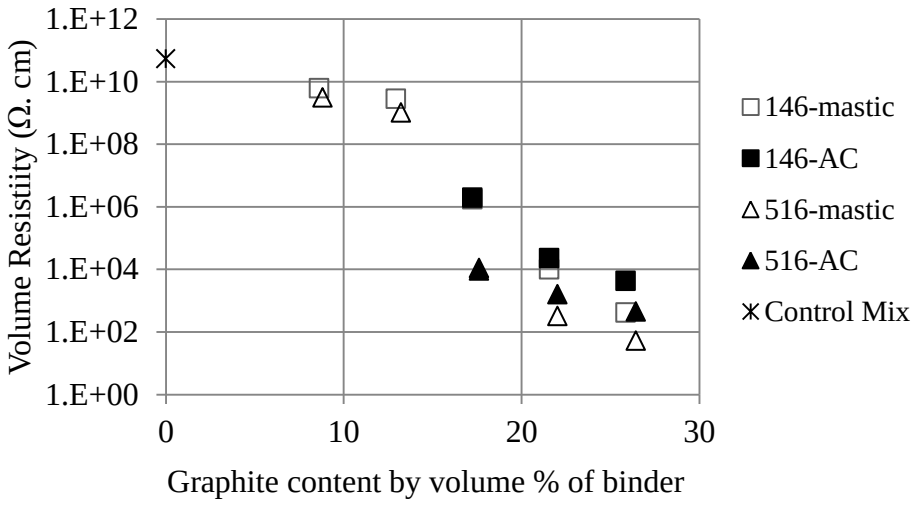

Figure 20. Volume resistivity versus graphite content for conductive asphalt concrete

Indirect Tensile Strength

IDT test is one of the common tests to characterize mechanical performance of asphalt concrete. IDT strengths were measured to investigate the effect of adding graphite on the mechanical performance. Figure 21 shows the average ITD strength obtained from three specimens for each case. The ITD strength of the control mixture is 1.12 MPa, and the strength increases with increase of graphite content. The maximum

improvement in ITD strength is 41% at the specimens containing 25% graphite by weight of asphalt mastic. Addition of more graphite in the mix resulted in decrease in ITD strength. It seems that adding graphite reduces the thickness of asphalt mastic film around the aggregates, which can have negative effect on mechanical performance. This result is similar to the ITD strength results of porous asphalt concrete containing steel fibers (Liu et al. 2010b). As shown in Figure 21, mechanical performance of F516 is better than F146.

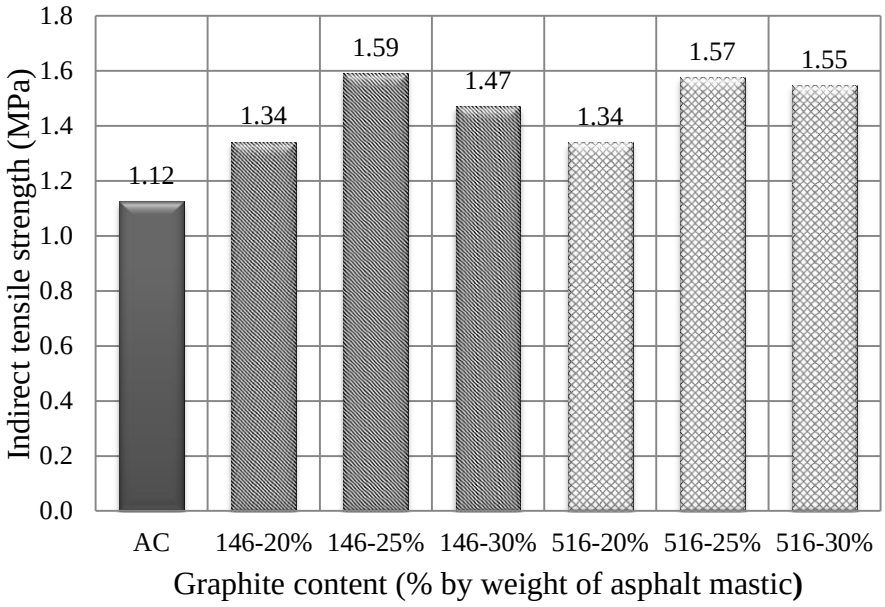

Figure 21. Effect of graphite contents on IDT strength of conductive asphalt concrete

Appendix A5 presents the load versus extension curve of IDT specimens along with a summary of all the IDT results obtained from this experiment.

Thus, addition of 25% (by weight of asphalt mastic) F516 to asphalt concrete has sufficiently low electrical resistivity ($1.6x10^3$ Ω.cm) and also improves the mechanical strength of the mix. Considering both efficiency in imparting conductivity and mechanical performance, it can be concluded that flake type F516 graphite is the best graphite for multifunctional applications.

6. CONCLUSION AND RECOMMENDATION

The effect of graphite on imparting electrical conductivity into asphalt concrete is investigated in this study. Electrical volume resistivity of the mastic specimens containing various types and contents of graphite is examined, and the physical explanations for their resistivity variation are suggested based on the SEM analysis for the graphite particles.

Major conclusions from the study are listed as follows:

- Volume resistivity of the asphalt mastics significantly vary with the graphite types;
- The graphite having flake shape particles improves the conductivity of the asphalt mixtures to a greater extent;
- Mixing difficulty is observed with high surface area graphite, which has particle size of 1.64 μm ;
- The flake type graphite improves the conductivity of asphalt concrete mixtures with similar trend to asphalt mastics;
- The conductive asphalt concrete containing flake type graphite fillers has improved IDT strength when compared to plain asphalt concrete;

Flake graphite 516 exhibits good electrical conductivity along with mechanical performance. The stepwise decrease in electrical resistivity of this conductive asphalt concrete can be utilized for various multifunctional applications as discussed in the previous chapters.

The effect of different binder grades on imparting conductivity in asphalt concrete and more mechanical tests such as resilient modulus, IDT ratio etc. are recommended for investigation in the future.

REFERENCES

Asbury Carbons (2013). "Materials", <http://www.asbury.com/Graphite.html>.

Asphalt Institute. (2001). *Superpave Mix Design*, Superpave Series No.2 (SP-2), Third Edition, Lexington, KY.

ASTM. (2001). "Standard specification for hot-mixed, hot-laid bituminous paving mixtures." *ASTM D3515-01*, West Conshohocken, PA.

ASTM. (2003). "Standard test method for theoretical maximum specific gravity and density of bituminous paving mixtures." *ASTM D2041-03,* West Conshohocken, PA.

ASTM. (2005). "Standard test method for percent air voids in compacted dense and open bituminous paving mixtures." *ASTM D3203-05,* West Conshohocken, PA.

ASTM. (2006). "Standard test method for sieve analysis of fine and coarse aggregates." *ASTM C136-06,* West Conshohocken, PA.

ASTM. (2007a). "Standard specification for performance graded asphalt binder." *ASTM D6373-07,* West Conshohocken, PA.

ASTM. (2007b). "Standard test method for bulk specific gravity and density of compacted bituminous mixtures using coated samples." *ASTM D1188-07*, West Conshohocken, PA.

ASTM. (2007c). "Standard test method for indirect tensile (IDT) strength of bituminous mixtures." *ASTM D6931-07,* West Conshohocken, PA.

Barnard, E. H. (1965). "Electrically conductive concrete." U.S. Patent 3,166,518.

Blackburn, R.R., Bauer, K. M., Amsler, Sr. D. E., Boselly III, S.E., and McElroy, A.D. (2004). *Snow and Ice Control: Guidelines for materials and methods*. NCHRP Report 526. Washington, DC: Transportation Research Board, National Cooperative Highway

Research Program.

Bonnaure, F. P., Huibers, A. H., and Boonders, A. (1982). "A laboratory investigation of the influence of rest periods on the fatigue characteristics of bituminous mixes." *Journal of the Association of Asphalt Paving Technologists*, 51, 104–128.

Chen, F., Chen, M., Wu, S., and Zhang, J. (2012). "Research on pavement performance of steel slag conductive asphalt concrete for deicing and snow melting." *Key Engineering Materials*, 509, 168-174.

Chung, D. D. L. (2003). *Multifunctional Cement-Based Materials*, Marcel Dekker, Inc., New York, NY.

Chung, D.D.L. and Wang, S. (2003). ''Self-sensing of damage and strain in carbon Fiber polymer-matrix structural composites by electrical resistance measurement,'' *Polymer & Polymer Composites*, 11(7), 515–525.

Daniel, J. S. and Kim, Y. R. (2001). "Laboratory evaluation of fatigue healing of asphalt mixtures." *Journal of Materials in Civil Engineering*, 13(6), 434-440.

Fromm, H. J. (1976). "Electrically conductive asphalt mixes for the cathodic protection of concrete bridge decks," *Proceedings of Association of Asphalt Paving Technol*ogists, 382-399.

García, A., Schlangen, E., Van de Ven, M., and Liu, Q. (2009). "Electrical conductivity of asphalt mortar containing conductive fibers and fillers." *Construction and Building Materials*, 23(10), 3175-3181.

García, A., Schlangen, E., Van de Ven, M., and Van Vliet, D. (2011). "Induction heating of mastic containing conductive fibers and fillers." *Materials and Structure*, 44, 499-508.

Gibson, R. F. (2010). "A review of recent research on mechanics of multifunctional composite materials and structures." *Composite Structures*, 92, 2793-2810.

Huang, B., Cao, J., Chen, X., Shu, X., and He, W. (2006). "Laboratory investigation into electrically conductive HMA mixtures." *Journal of the Association of Asphalt Paving Technologists*, 75, 1235-1253.

Huang, B., Chen, X., and Shu, X. (2009). "Effects of electrically conductive additives on laboratory-measured properties of asphalt mixtures." *Journal of Materials in Civil Engineering*, 21, 612-617.

Lee, K. W. and Correia, A.J. (2010). *A pilot study for investigation of novel methods to harvest solar energy from asphalt pavements*, A Final Report for Korea Institute of Construction Technology (KICT), University of Rhode Island, Kingston, RI.

Lofgren, S. (2001). "The chemical effects of deicing salt on soil and stream water of five catchments in southeast Sweden." *Water, Air, and Soil Pollution*, 130, 863-868.

Little, D. N. and Bhasin, A. (2007). "Exploring mechanism of healing in asphalt mixtures and quantifying its impact." *Self healing materials an alternative approach to 20 centuries of materials science*, 100, 205-218.

Liu, Q., Schlangen, E., Ven, M., and Poot, M. (2010a). "Optimization of steel fiber used for induction heating in porous asphalt concrete." *Proceedings of the Seventh International Conference on Traffic and Transportation Studies, ASCE, Kunming, China, August 3-5*, 1320–1330.

Liu, Q., Schlangen, E., García, A., and Ven, M. (2010b). "Induction heating of electrically conductive porous asphalt concrete." *Construction and Building Materials*, 24(7), 1207-1213.

Liu, Q., Schlangen, E., Ven, M., and Garcia, A. (2010c). "Healing of porous asphalt concrete via induction heating." *Road Materials and Pavement Design*, 11(S1), 527-542.

Liu, X., Wu, S., Ning, L., and Bo, G. (2008). "Self-monitoring application of asphalt concrete containing graphite and carbon fibers." *Materials Science Edition*, 23(2), 268-271.

Liu, X. and Wu, S. (2009). "Research on the conductive asphalt concrete's piezoresistivity effect and its mechanism." *Construction and Building Materials*, 23(8), 2752-2756.

Liu, X. and Wu, S. (2011a). "Study on the graphite and carbon fiber modified asphalt concrete." *Construction and Building Materials*, 25, 1807-1811.

Liu, X. and Wu, S. (2011b). "Study on the piezoresistivity character of electrically conductive asphalt concrete." *Advanced Materials Research*, 233-235, 1756-1761.

Mallick, R. B., Chen. B. L., Bhowmick, S., and Hulen, M. S. (2008). "Capturing solar energy from asphalt pavements." *Proceedings of International ISAP Symposium on Asphalt pavements and Environment*, International Society for Asphalt Pavements (ISAP), Zurich, Switzerland, August 18-20, 2008.

Mo, L., Wu, S., Liu, X., and Chen, Z. (2005). "Percolation model of graphite-modified asphalt concrete." *Journal of Wuhan University of Technology Mater. Sci. Ed.*, 20(1), 111-113.

Minsk, L. D. (1968). "Electrically conductive asphalt for control of snow and ice accumulation." *Highway Research Record*, 227, 57-63.

Minsk, L. D. (1971). "Electrically conductive asphaltic concrete." U.S. Patent 3,573,427.

Park, P. (2012). *Characteristics and applications of high-performance fiber reinforced asphalt concrete*. Ph.D. Dissertation, University of Michigan, Ann Arbor, MI.

Sanzo, D. and Hecnar, S., J. (2006). "Effects of road de-icing salt (NaCl) on larval wood frogs." *Environmental Pollution*, 140, 247-256.

Serin, S., Morova, N., Saltan, M., and Terzi, S. (2012). "Investigation of usability of steel fibers in asphalt concrete mixtures." *Construction and Building Materials*, 36, 238-244.

Stratfull, R. F. (1974). "*Experimental Cathodic Protection of a Bridge Deck*," Highway Research report, California Department of Transportation, Report No. CA_DOT-TL-5117-4-74-02.

Wen, S. and Chung, D. D. L. (2007). "Electrical resistance based damage self-sensing in carbon fiber-reinforced cement." *Carbon*, 45(4), 710-716.

Wu, S., Liu, X., Ye, Q., and Li, N. (2006). "Self-monitoring electrically conductive asphalt-based composite containing carbon fillers." *Transactions of Nonferrous Metals Society of China*, 16(S2) 512-516.

Wu, S., Mo, L., and Shui, Z. (2003). "Piezoresistivity of graphite modified asphalt-based composites." *Key Engineering Materials*, 249, 391-396.

Wu, S., Mo, L., Shui, Z., and Chen, Z. (2005). "Investigation of the conductivity of asphalt concrete containing conductive fillers." *Carbon*, 43(7), 1358–1363.

Wu, S., Zhang, Y., and Chen, M. (2010). "Research on mechanical characteristics of conductive asphalt concrete by indirect tensile test." *Proceedings of Fourth International conference on Experimental Mechanics*, Wuhan, China.

Xiangyang, W. and Yuxing, G. (2010). “Research on the preparation of conductive asphalt concrete for deicing and snow melting.” *Proceedings of 3rd Internation Conference on Advanced Computer Theory and Engineering*, 381-384.

Zaleski, P. L., Derwin, D. J., and Flood, W. H. (1998). “Electrically conductive paving mixture and paving system.” U.S. Patent 5,707,171.

APPENDIX

A1. Electrical Resistivity of Asphalt Mastics Containing Various Graphite Types

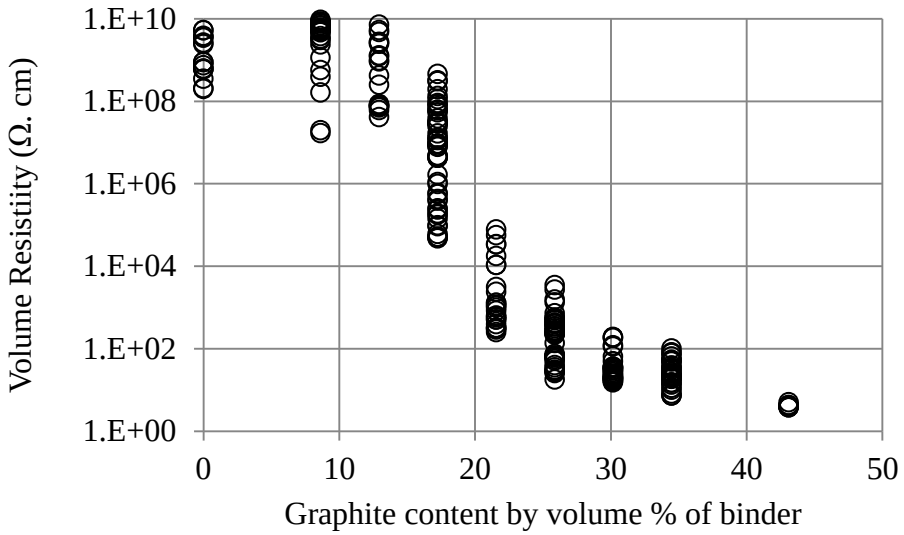

Figure 22. Variation in volume resistivity with F146 graphite contents

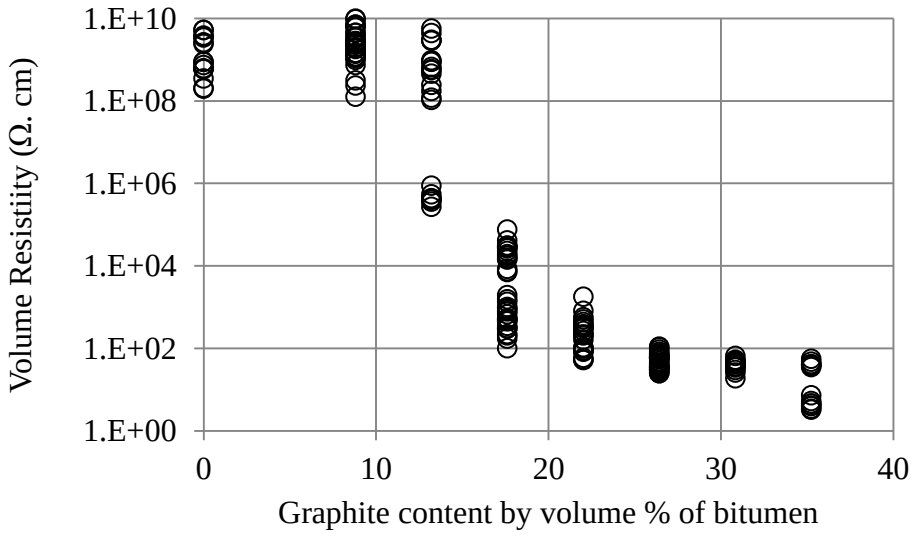

Figure 23. Variation in volume resistivity with F516 graphite contents

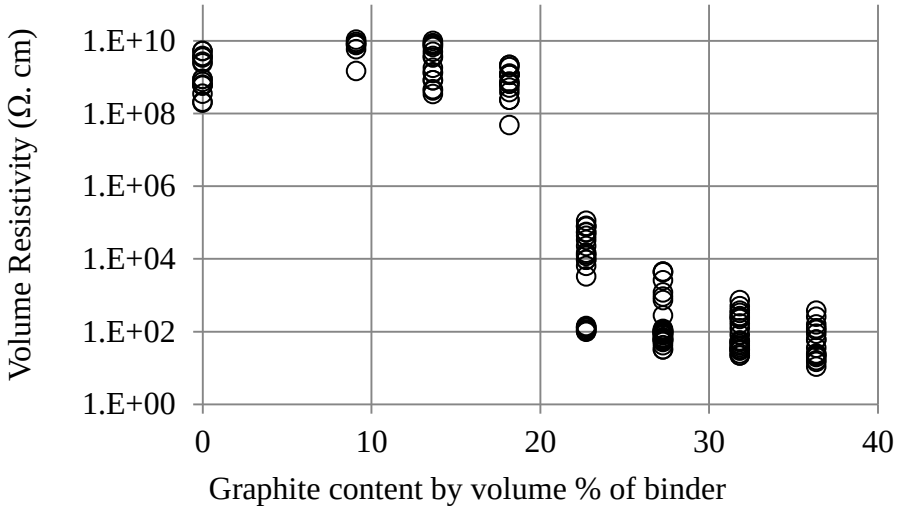

Figure 24. Variation in volume resistivity with F3204 graphite contents

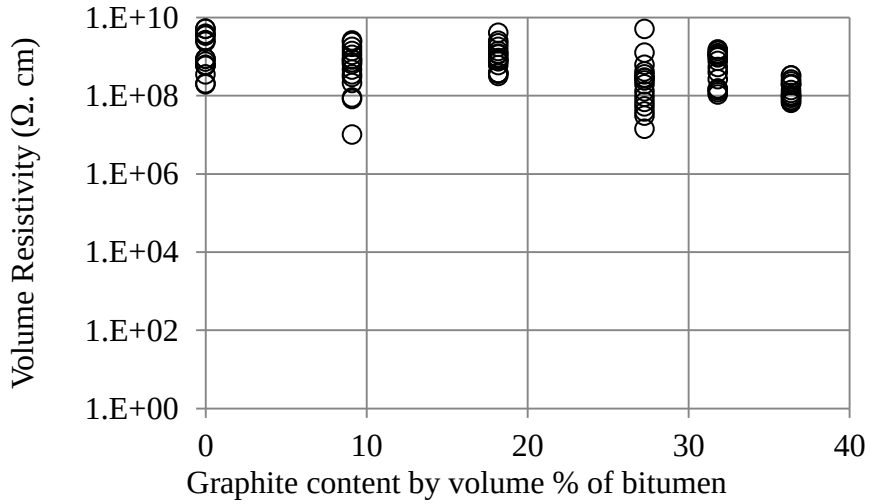

Figure 25. Variation in volume resistivity with 505 graphite contents

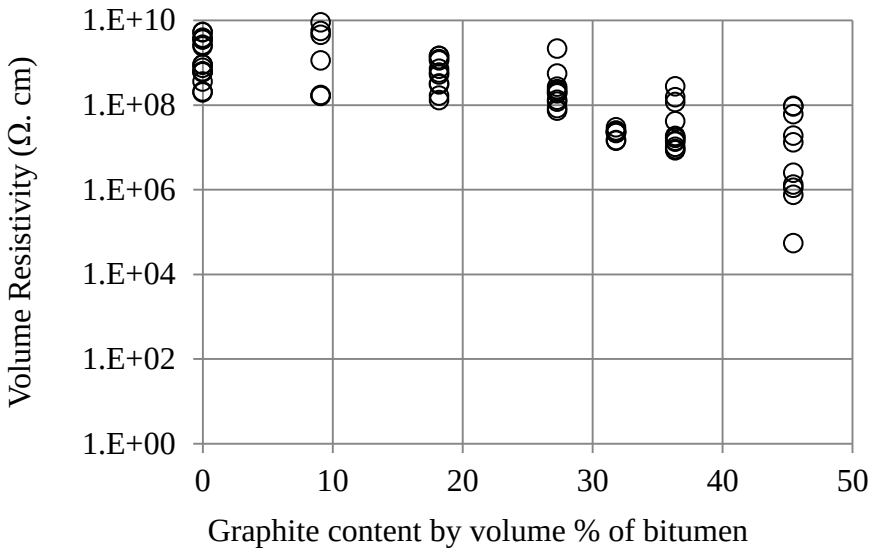

Figure 26. Variation in volume resistivity with 508 graphite contents

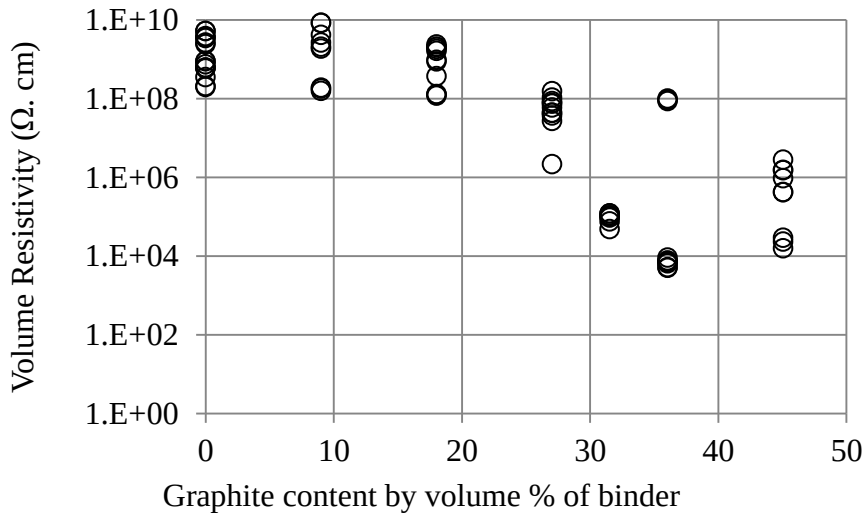

Figure 27. Variation in volume resistivity with A99 graphite contents

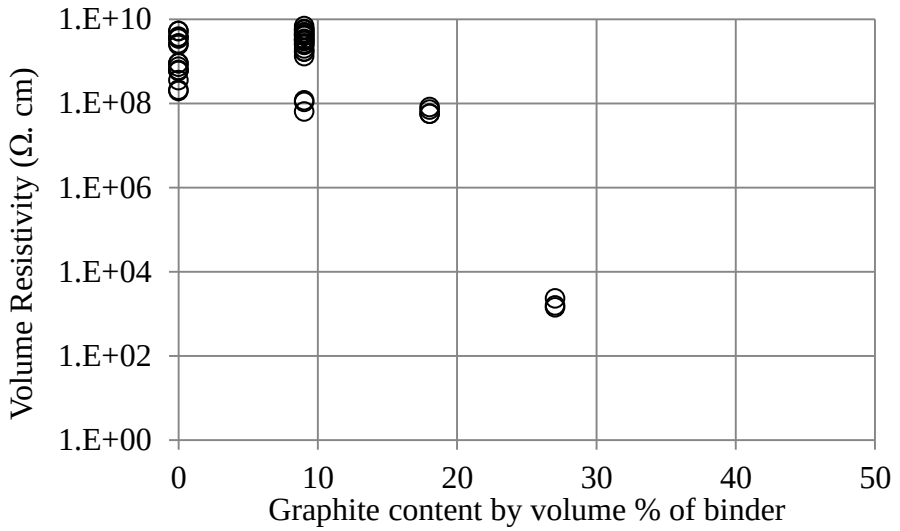

Figure 28. Variation in volume resistivity with SA4827 graphite contents

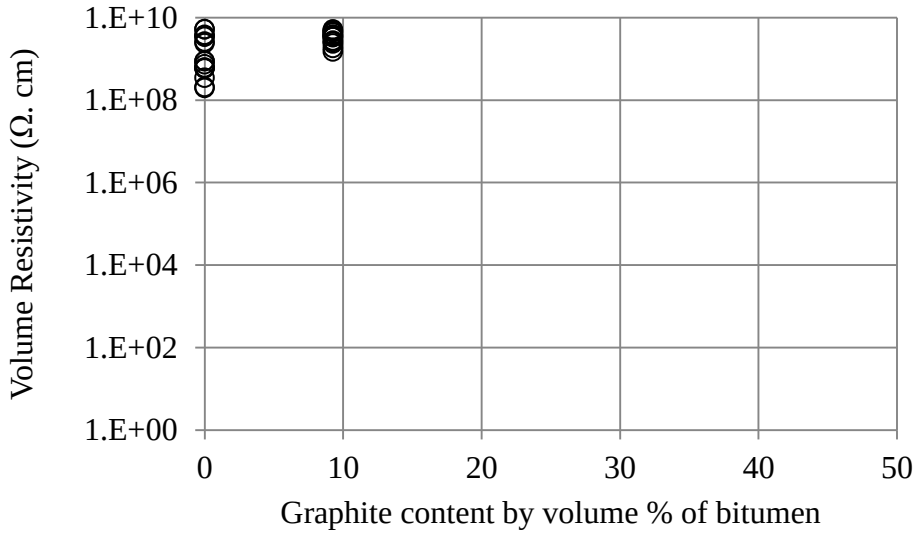

Figure 29. Variation in volume resistivity with TC307 graphite contents

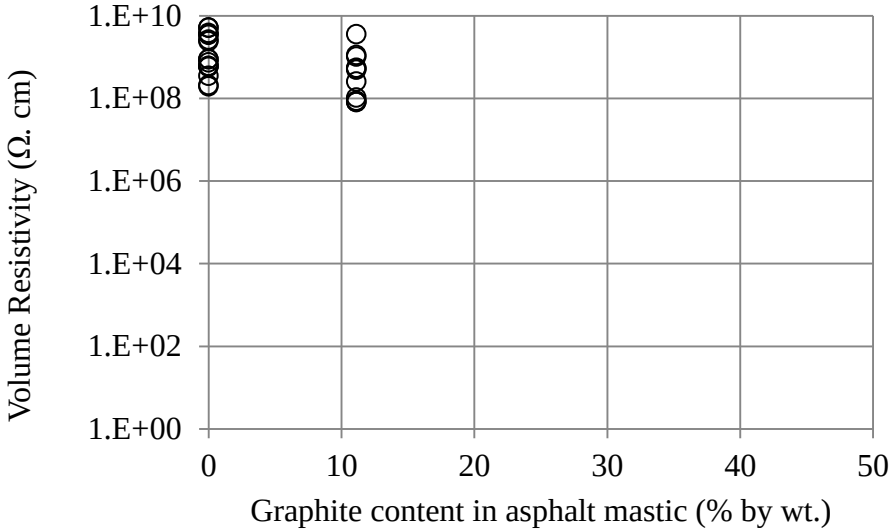

Figure 30. Variation in volume resistivity with 5303 graphite contents

A2. Sieve Analysis of Aggregates

Table 7. Sieve analysis of coarse aggregate

Sieve Size	*Sieve size (mm)*	*Mass sieve (g)*	*Mass sieve+agg.(g)*	*Mass retained (g)*	*Total % retained*	*Total % passing*
3/4"	19	794	794	0	0	100
1/2"	12.5	787	789.5	2.5	0.17	99.83
3/8"	9.5	804.5	1003.5	199	13.43	86.57
#4	4.75	777	1939.5	1162.5	90.93	9.07
#8	2.36	717	840.5	123.5	99.17	0.83
#16	1.18	630.5	634	3.5	99.40	0.60
Pan	0	383	392	9	100.00	0.00

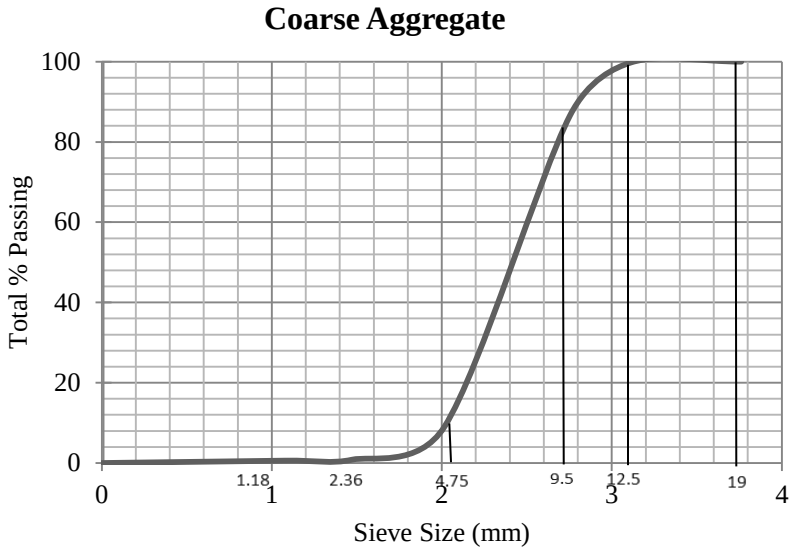

Figure 31. Gradation of coarse aggregate

Table 8. Sieve analysis of fine aggregate

Sieve Size	*Sieve size (mm)*	*Mass sieve (g)*	*Mass sieve+agg.(g)*	*Mass retained (g)*	*Total % retained*	*Total % passing*
3/8"	9.5	804.5	804.5	0	0	100
#4	4.75	777	778.5	1.5	0.10	99.90
#8	2.36	717	1079	362	24.23	75.77
#16	1.18	630.5	1016	385.5	49.93	50.07
#30	0.6	575	925.5	350.5	73.30	26.70
#50	0.3	545.5	782.5	237	89.10	10.90
#100	0.15	529	636.5	107.5	96.27	3.73
#200	0.075	294	323.5	29.5	98.23	1.77
Pan	0	383	409.5	26.5	100.00	0.00

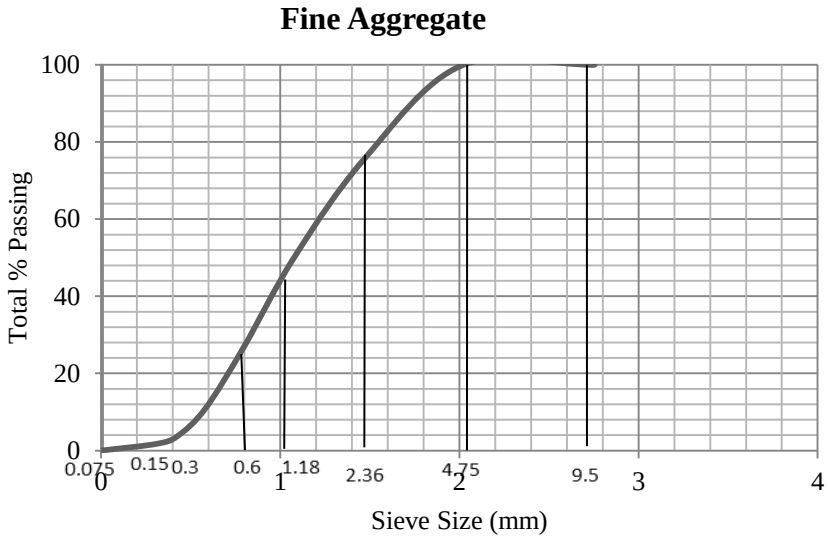

Figure 32. Gradation of fine aggregate

Table 9. Sieve analysis of aggregate (ASTM 2006)

Sieve size (mm)	*% Passing CA*	*% Passing FA*	*% Passing Filler*	*Gradation (0.35/0.6/0.05)*	*Specification D-6 mix*
19	100	100	100	100.0	
12.5	99.83	100	100	99.9	100
9.5	86.57	100	100	95.3	90-100
4.75	9.07	99.90	100	68.1	55-85
2.36	0.83	75.77	100	50.8	32-67
1.18	0.60	50.07	100	35.3	
0.6	0.00	26.70	100	21.0	
0.3	0.00	10.90	100	11.5	7-23
0.15	0.00	3.73	100	7.2	
0.075	0.00	1.77	100	6.1	2-10

Nominal maximum size: One sieve size larger than the first sieve to retain more than 10 percent – **9.5 mm**

Maximum size: One sieve size larger than the nominal maximum size – **12.5 mm**

A3. Determination of Binder Content: 5.3 % for 4% Air Void

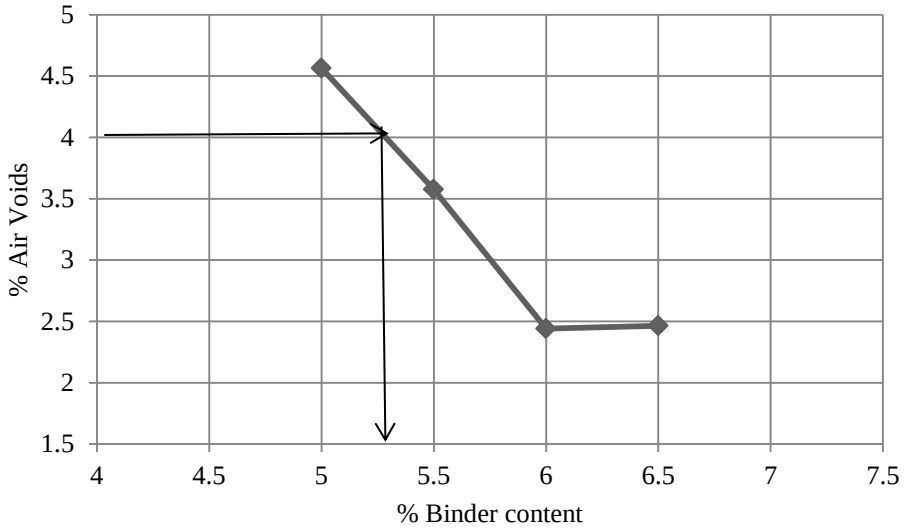

Figure 33. Air voids versus % binder content

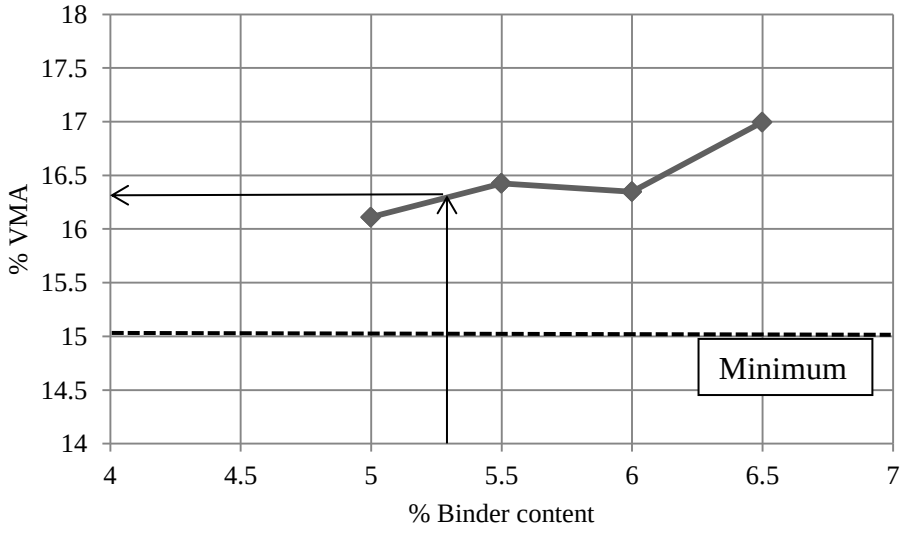

Figure 34. VMA versus % binder content

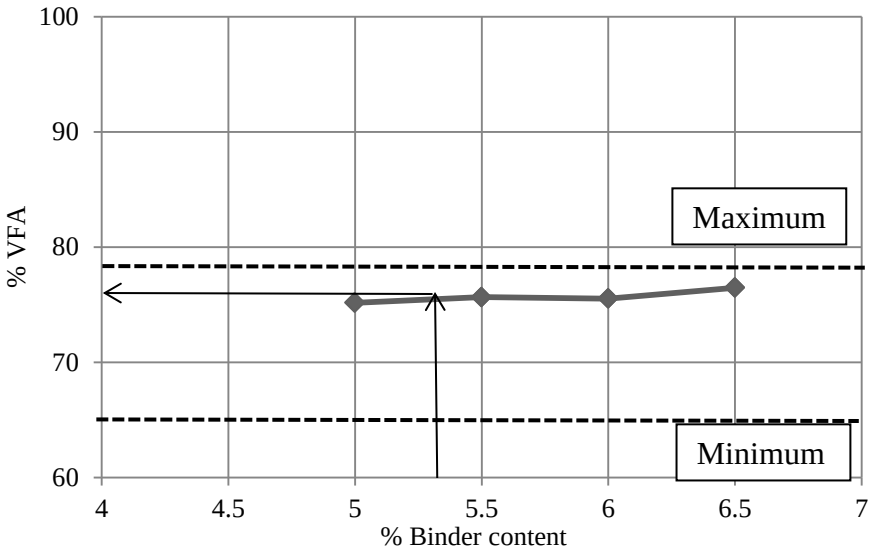

Figure 35. VFA versus % binder content

A4. Electrical Resistivity of Conductive Asphalt Concrete

Table 10. Electrical resistivity of conductive asphalt concrete

Specimen	Resistance (Ω)	Volume resistivity (Ω. cm)
Control mix		
1	3.22E+10	6.00E+10
2	3.41E+10	6.37E+10
3	2.02E+10	3.77E+10
146-20%		
1	9.68E+05	1.80E+06
2	1.06E+06	1.98E+06
3	1.08E+06	2.00E+06
146-25%		
1	1.48E+04	2.77E+04
2	1.04E+04	1.94E+04
3	1.11E+04	2.06E+04
146-30%		
1	2.09E+03	3.89E+03
2	2.64E+03	4.93E+03
3	2.13E+03	3.96E+03
516-20%		
1	2.94E+03	5.48E+03
2	4.77E+03	8.89E+03
3	6.98E+03	1.30E+04
516-25%		
1	9.08E+02	1.69E+03
2	9.25E+02	1.73E+03
3	7.37E+02	1.37E+03
516-30%		
1	2.32E+02	4.33E+02
2	2.02E+02	3.76E+02
3	2.92E+02	5.44E+02

A5. Indirect Tensile Strength Test Results

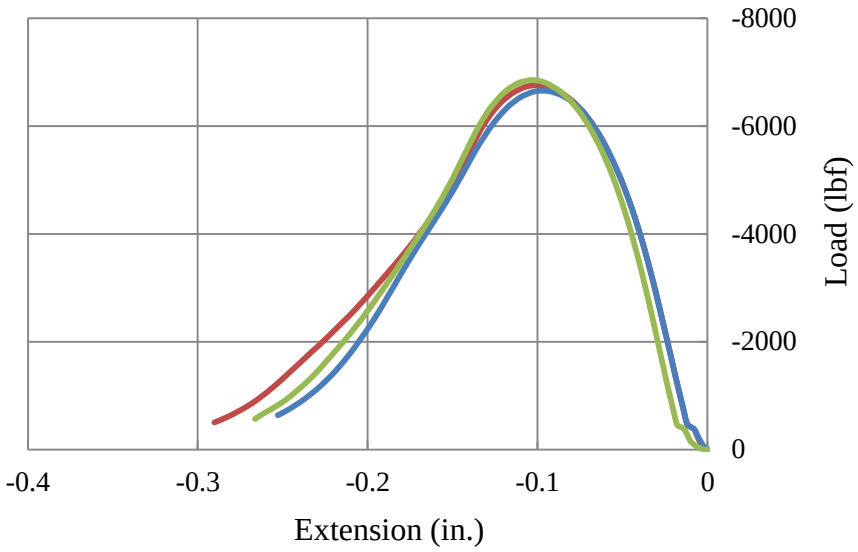

Figure 36. Load versus extension curve of IDT test for F146-20%

Table 11. IDT strength of various graphite contents

Sample	*Load (lbf)*	*Load- P (N)*	S_T *(MPa)*
Cement	5641.61	25095.0096	1.12169
	5225.79	23245.3591	1.03901482
	6100.504	27136.2619	1.21292935
F146-20%	6656.996	29611.6496	1.32357357
	6720.207	29892.8248	1.33614146
	6854.619	30490.7162	1.36286585
F146-25%	7852.357	34928.8544	1.56124056
	8237.095	36640.246	1.63773588
	7909.71	35183.972	1.57264374
F146-30%	1556.657	6924.32167	---
	6965.326	30983.1631	1.38487711
	7822.166	34794.5588	1.55523785
F516-20%	6392.453	28434.9094	1.27097595
	7179.32	31935.0512	1.42742435
	6617.187	29434.5712	1.31565856
F516-25%	7708.553	34289.1855	1.53264881
	8688.312	38647.3494	1.72744885
	7360.641	32741.6033	1.4634754
F516-30%	7554.681	33604.732	1.50205529
	7538.183	33531.3456	1.49877509
	8222.955	36577.3484	1.6349245

1 lbf = 4.448 N

$$S_T = \frac{2 \text{ X } P}{\pi \text{ X } t \text{ X } D}$$

where, t = 95 mm and D = 150 mm.